NP-12592
Report Number

United States Atomic Energy Commission
Division of Technical Information

OTI-131(May 1962)

14 #1.

15 35717

(19) TR 62-661.7

NP 12592

(1) EXPERIMENTAL STUDY OF FACTORS CONTROLLING THE EFFECTIVENESS OF HIGH-TEMPERATURE PROTECTIVE COATINGS FOR TUNGSTEN,

(11) by M. G. Nicholas, C. D. Dickinson, L. L. Seigle

Issued December 15, 1962

(9) Second Quarterly Progress Report

(15) Contract AF 33(657)-8287

August 15 - November 15, 1962

Submitted to

AFSC, AERONAUTICAL SYSTEMS DIVISION
WRIGHT-PATTERSON AIR FORCE BASE, OHIO

GENERAL TELEPHONE & ELECTRONICS LABORATORIES
INCORPORATED

BAYSIDE LABORATORIES, BAYSIDE, NEW YORK

(7) I
(12) V
(13) NA
(16) NA
(17) NA
(18) NA
(19) NA
(4) UL
(21) NA

L1,C

GENERAL TELEPHONE & ELECTRONICS LABORATORIES

ABSTRACT

Two processes governing the efficacy of high-temperature protective coatings for tungsten, interdiffusion in ternary oxygen-metal-metal systems and breakaway during oxide film growth, are being investigated experimentally to determine the oxidation behavior of binary alloys and the influence of substrate mechanical properties on the growth characteristics of the oxide films. Experiments involving oxidation kinetics and the microstructural and quantitative identification of the layers formed have been conducted on four systems. An analysis of the diffusion processes governing growth in the Zr-Th-O system is presented, and a preliminary discussion of the results obtained in the W-Hf-O, ZrN-ThN-O and Sn-Al-Cr systems is given.

-A-

-A-

TABLE OF CONTENTS

	5.3 Future Studies	49
6.	SELECTION OF FUTURE SYSTEMS	49
	REFERENCES	51
	APPENDIX	

1. INTRODUCTION

The object of this program is to improve our knowledge and understanding of the factors controlling the efficacy of oxidation-resistant coatings for tungsten at temperatures of 2000°C and above. An analysis of the behavior of existing high-temperature coatings, conducted by these Laboratories under Contract AF 33(616)-8175, led to the definition of five processes as being of major importance in determining the protectiveness of a coating system:

1. Breakaway, or the change from "parabolic" to "linear" oxide film growth. This phenomenon is accompanied by destruction of the protective character of the oxide film.
2. Multicomponent diffusion-controlled reactions leading to a specific sequence and morphology of oxide and other phases at the air-coating interface. In many practical systems two metal components as well as oxygen are involved, and this process is referred to, for convenience, as "ternary diffusion."
3. Loss of material by evaporation of the coating or substrate, or by the formation of volatile oxidation products.
4. Interactions between the coating and the protected substrate.
5. Diffusion through the oxide film. When the film is protective, the rates of cation and/or anion diffusion control the progress of the oxidation reaction.

The first of these five processes, breakaway, is believed to be the most important, since no coating is really protective unless it forms a coherent outer oxide film. Previous work in these Laboratories under Contract AF 33(616)-8175 showed that the mechanical properties of the substrate

4. Interactions between the coating and the protected substrate.
5. Diffusion through the oxide film. When the film is protective, the rates of cation and/or anion diffusion control the progress of the oxidation reaction.

The first of these five processes, breakaway, is believed to be the most important, since no coating is really protective unless it forms a coherent outer oxide film. Previous work in these Laboratories under Contract AF 33(616)-8175 showed that the mechanical properties of the substrate

influence breakaway and, in particular, that the use of a liquid substrate

delays its onset during the growth of HfO_2, ZrO_2 and ThO_2 films. One objective of the present program is to extend this preliminary study by evaluating (1) the influence of liquid substrates on the growth of complex refractory oxides, and (2) the effect of solid substrate mechanical properties on the growth of simple refractory oxides. For these purposes, the oxidation of liquid Sn-Al-Cr alloys and the oxidation of thorium-zirconium nitrides are being studied.

A second objective of the program is to increase our understanding of the rules governing the sequence and morphology of phases formed at the air-coating interface by reaction of the coating with oxygen, i.e. of the "ternary diffusion" process. The success of a coating depends primarily upon its ability to form a particular surface oxide of the several that might be produced. As explained in the first progress report, the sequence of oxide and other layers at the surface depends upon complex diffusional, as well as thermodynamic, factors, the details of which are not yet completely understood. Some progress has been made in rationalizing the influence of multicomponent diffusion on the sequence and morphology of phases in ternary metal systems by Clark and Rhines, and by Kirkaldy. It is our objective to apply and extend this knowledge to representative ternary metal-oxygen systems of potential significance for ultra-high temperature coatings. The systems chosen for this purpose are Th-Zr-O and W-Hf-O.

During the second quarter, main emphasis has been placed upon continuing investigations of the oxidation of Th-Zr alloys; the results of this work will be reported first. Studies of the oxidation behavior of W-Hf alloys and thorium-zirconium nitrides have also continued and are presented later. In addition, an investigation of the oxidation of liquid Sn-Al-Cr alloys was initiated and is discussed last.

metal-oxygen systems of potential significance for ultra-high temperature coatings. The systems chosen for this purpose are Th-Zr-O and W-Hf-O.

During the second quarter, main emphasis has been placed upon continuing investigations of the oxidation of Th-Zr alloys; the results of this work will be reported first. Studies of the oxidation behavior of W-Hf alloys and thorium-zirconium nitrides have also continued and are presented later. In addition, an investigation of the oxidation of liquid Sn-Al-Cr alloys was initiated and is discussed last.

2. THE THORIUM-ZIRCONIUM-OXYGEN SYSTEM

2.1 EXPERIMENTAL PROCEDURE

The reasons for selecting the Th-Zr-O system for study of the "boronry diffusion" process were explained in the First Quarterly Progress Report on this contract. During the first quarter, alloys containing 30, 45, 70, and 85% Th were fabricated as sheet, and oxidation behavior at 750°, 1000° and 1400°C in air was studied. During the second quarter, the oxidation behavior of these alloys at 1000, 1200, 1400, and 1600°C has been further investigated. Weight gain, oxide thickness measurements and metallographic studies were carried out in the General Telephone & Electronics Laboratories. Details of the experimental procedure are given in the First Quarterly Report.

In recent sequential tests in which one specimen was weighed and reheated for several oxidation rate measurements, it was found that thermal cycling caused spalling of the oxide and anomalies in the oxidation rate measurements at 1400°C and above. To obtain valid oxidation rate measurements at these high temperatures, duplicate tests were conducted on individual specimens oxidized without reheating. Microprobe and x-ray analysis of the complex oxide layers formed on the alloys are being carried out by Battelle Memorial Institute. The experimental procedures used by Battelle are described in Appendix I of this report. Analysis of the alloys oxidized for 1/2 hour at 1200°C has been completed and the [illegible] examination [illegible].

2.2 RESULTS

2.2.1 Rate of Oxidation

The rate of oxidation was determined by measuring the weight gain of the specimens after exposure at 750, 1000, 1200, 1400 and 1600°C. The results for each alloy are shown in Figs. 1 to 4, and the type of test used is indicated. In these figures, the log of the specific weight gain is plotted as a function of the log of time and the slope of the resulting curve is the index of reaction, n, in the equation

$$\frac{\Delta W}{A} = kt^n . \qquad (1)$$

In almost all cases, the data for both non-cyclic and cyclic tests for a given temperature and composition are well described by a straight line with a slope of 1 or 1/2, indicating nonprotective (linear) or protective (parabolic) film growth, respectively. The rate constants presented in Table I were determined from the straight lines of $\Delta W/A$ vs t^n plots by assuming that either linear (n=1) or parabolic ($n=\frac{1}{2}$) growth best describes the kinetics of the oxidation reaction.

At 750 and 1000°C linear oxidation was observed on all compositions tested, and the oxide formed was externally cracked. The tests were sequential cyclic runs on one sample, but cracking apparently occurred even on the first run as indicated by the fact that for the alloys containing 70-85%Th, the weight gained at 1000°C in the initial run is greater than [illegible]

2. THE THORIUM-ZIRCONIUM-OXYGEN SYSTEM

2.1 EXPERIMENTAL PROCEDURE

The reasons for selecting the Th-Zr-O system for study of the "ternary diffusion" process were explained in the First Quarterly Progress Report on this contract. During the first quarter, alloys containing 30, 55, 70, and 85% Th were fabricated as sheet, and oxidation behavior at 750°, 1200° and 1600°C in air was studied. During the second quarter, the oxidation behavior of these alloys at 1000, 1200, 1400, and 1600°C has been further investigated. Weight gain, oxide thickness measurements and metallographic studies were carried out in the General Telephone & Electronics Laboratories. Details of the experimental procedure are given in the First Quarterly Report.

In recent sequential tests in which one specimen was weighed and reheated for several oxidation rate measurements, it was found that this thermal cycling caused spalling of the oxide and anomalies in the oxidation rate measurements at 1400°C and above. To obtain valid oxidation rate measurements at these high temperatures, duplicate tests were conducted on individual specimens oxidized without reheating. Microprobe and x-ray analysis of the complex oxide layers formed on the alloys are being carried out by Battelle Memorial Institute. The experimental procedures used by Battelle are described in Appendix I of this report. Analysis of the alloys oxidized for 1/2 hour at 1200°C has been completed and the following additional samples submitted to Battelle:

1. Zr-30%Th, oxidized 2 hours at 1200°C
2. Zr-85%Th, oxidized 2 hours at 1200°C
3. Zr-30%Th, oxidized 20 minutes at 1400°C.

2.2 RESULTS

2.2.1 Rate of Oxidation

The rate of oxidation was determined by measuring the weight gain of the specimens after exposure at 750, 1000, 1200, 1400 and 1600°C. The results for each alloy are shown in Figs. 1 to 4, and the type of test used is indicated. In these figures, the log of the specific weight gain is plotted as a function of the log of time and the slope of the resulting curve is the index of reaction, n, in the equation

$$\frac{\Delta W}{A} = kt^n . \qquad (1)$$

In almost all cases, the data for both non-cyclic and cyclic tests for a given temperature and composition are well described by a straight line with a slope of 1 or 1/2, indicating nonprotective (linear) or protective (parabolic) film growth, respectively. The rate constants presented in Table I were determined from the straight lines of $\Delta W/A$ vs t^n plots by assuming that either linear (n=1) or parabolic ($n=\frac{1}{2}$) growth best describes the kinetics of the oxidation reaction.

At 750 and 1600°C linear oxidation was observed on all compositions tested, and the oxide formed was externally cracked. The tests were sequential cyclic runs on one sample, but cracking apparently occurred even on the first run as indicated by the fact that for the alloys containing 70-85%Th, the weight gained at 1000°C in the initial run is greater than that gained at 1200°C in the same time.

At 1200°C individual specimens were used for each test and the data can be represented by a line with $n=\frac{1}{2}$, indicating parabolic growth. The scales appeared to be sound and dense, and the edges and corners were intact in most cases; a sharp corner was retained in the oxide.

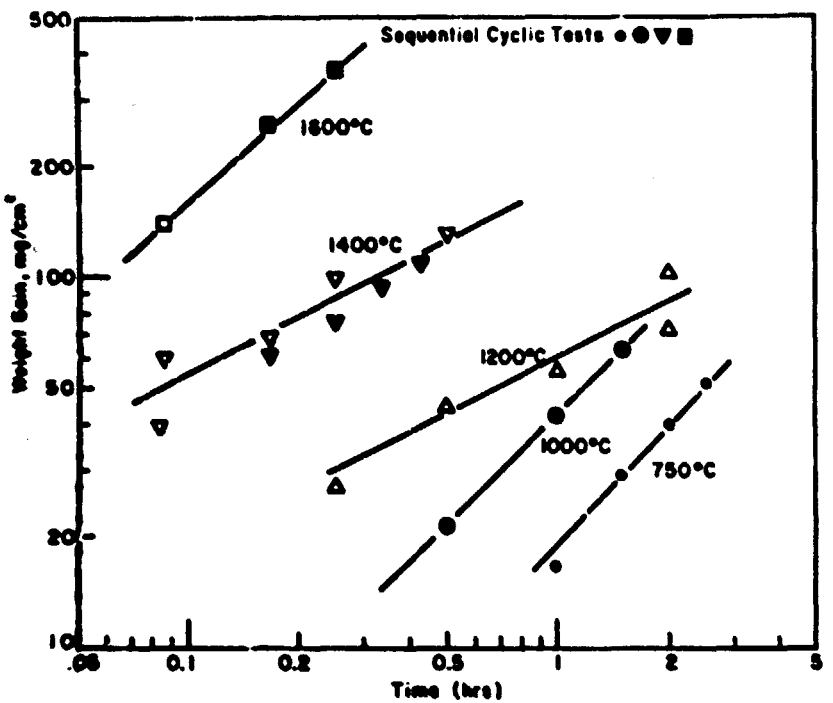

Fig 1. Weight gained in oxidation of Zr-30%Th sheet in dry air.

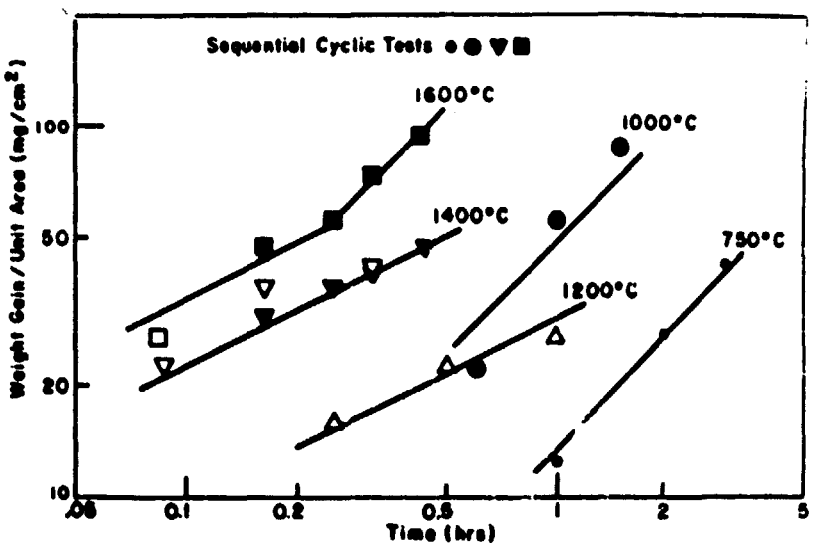

Fig. 2. Weight gained in oxidation of Zr-55%Th sheet in dry air.

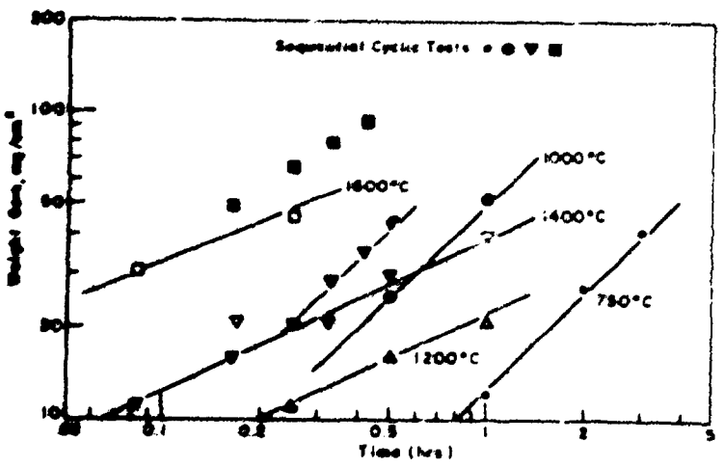

Fig. 3. Weight gained in oxidation of Zr-10%Th sheet in dry air.

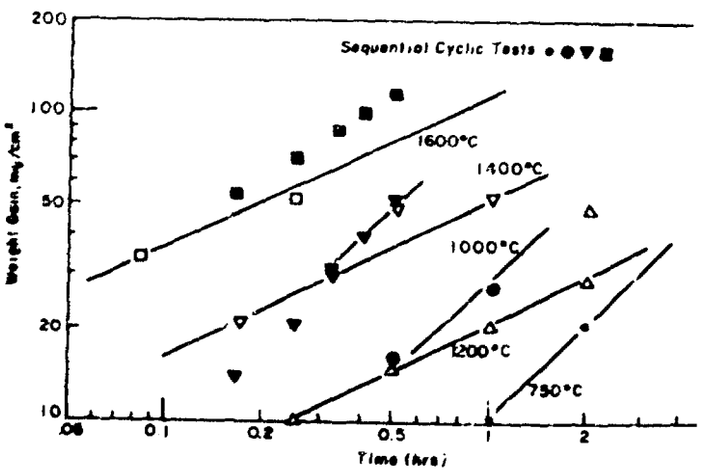

Fig. 4. Weight gained in oxidation of Zr-85%Th sheet in dry air.

TABLE I

The Effect of Temperature and Composition on the Growth Rate in Oxidation of Zr-Th Alloys at 750°C to 1600°C

	Zr-30% Th		Zr-55% Th		Zr-70% Th		Zr-85% Th	
Temp. (°C)	K_ℓ* gm/cm²/hr	K_p** gm²/cm⁴/hr	K_ℓ*	K_p**	K_ℓ*	K_p**	K_ℓ*	K_p**
750	2.4×10^{-2}	--	1.5×10^{-2}	--	2.3×10^{-2}	--	2.2×10^{-2}	--
1000	4.2×10^{-2}	--	5.7×10^{-2}	--	5.2×10^{-2}	--	2.9×10^{-2}	--
1200	--	3.14×10^{-3}	--	9.6×10^{-4}	--	4.3×10^{-4}	--	4.3×10^{-4}
1400	--	3.2×10^{-2}	--	6.7×10^{-3}	--	1.6×10^{-3}	--	2.92×10^{-3}
1600	1.7	--	(2.2×10^{-1})	1.02×10^{-2}	--	6.10×10^{-3}	--	1.3×10^{-2}

*K_ℓ = linear growth rate constant, i.e., $n \approx 1$ in $\frac{1}{n} \log \frac{\Delta W}{A} = \log Kt$.

**K_p = parabolic growth rate constant, i.e., $n \approx \frac{1}{2}$ in $\frac{1}{n} \log \frac{\Delta W}{A} = \log Kt$.

At 1400°C both cyclic and individual tests were run and in the Zr-30Th and Zr-55Th alloy, a line with n = 1/2 describes the results of both types of tests. In the Zr-70%Th alloy at 1400°C, the weight gains for individual specimen tests indicate a slope of 1/2 (Fig. 3), but in sequential tests beyond 0.25 hours the slope changes toward a linear rate, indicating breakaway. In the Zr-85%Th alloy only the individual tests fit a line with n = 1/2; the cyclic results indicate breakaway oxidation with n = 1. The external appearance of the oxides formed at 1400°C was similar to that observed at 1200°C.

At 1600°C only the Zr-30%Th alloy is solid at temperature. In the cyclic tests, the rate of weight gain on the liquid Zr-(70-85%)Th alloys is parabolic, but slopes of 0.68 were obtained for cyclic tests. In the solid Zr-30%Th alloy only cyclic tests were run, and a slope of 1 was observed (Fig. 1). The results of oxidation of the Zr-55%Th alloy can be described by a curve (Fig. 2) with an initial slope of 1/2 and a slope of 1 for times greater than 0.25 hr. The oxides formed at 1600°C appeared to be dense and sound, but on standing at room temperature the oxides formed on the liquid alloys disintegrated in the atmosphere to form a very fine powder.

2.2.2 Structure of the Surface Zone

2.2.2.1 Metallographic Studies

Metallographic examination reveals that at 750 and 1000°C, oxidation of all alloys proceeds by linear non-protective growth and the oxide formed contains a large number of cracks parallel to the surface of the specimen. As indicated in the last Quarterly Report, examination of the metallic substrate of specimens oxidized at 750°C indicates no change in substrate structure, and microhardness tests indicate no increase in

hardness of the metal adjacent to the metal-oxide interface. Thus the amount of oxygen which penetrates or dissolves in the substrate must be relatively small. At 750 and 1000°C, breakaway due to fracture of the oxide is evidently the controlling process in the rate of oxidation. Oxygen permeates through the cracks to the metal-oxide interface, forming new oxide which, in turn, spalls and does not protect the substrate. Under these conditions, the substrate is oxidized essentially in situ and solid-state diffusion processes do not control the composition of the oxide layer.

Cross-sections through the surface layers of samples that exhibited parabolic growth at 1200 and 1400°C were studied. The thickness of the layers formed is given in Table II. The microstructures after 1 hour in air at 1200°C were reported in the previous report. Photomicrographs of the structures of the Zr-30%Th and Zr-85%Th alloys after 2 hours at 1200°C are shown in Fig. 5, and of the Zr-55%Th alloys oxidized for 20 and 25 minutes at 1400°C, in Fig. 6

In general, the structures in Fig. 5 represent the two types of structures observed in samples oxidized at 1200 and 1400°C. At 1200 and 1400°C, the rate of growth is apparently diffusion-controlled in all compositions and compact adherent oxides are formed; however, the layers and structures observed in the Zr-30%Th and Zr-55%Th alloys (thorium lean) differ from those in the Zr-70%Th and Zr-85%Th (thorium rich) alloys. In the thorium lean alloys, several layers which thicken with time are observed as follows:

1. An external two-phased oxide,
2. An internally oxidized layer consisting of a single-phase metal matrix containing oxide particles,
3. A transformed two-phase metal matrix containing oxides formed by internal oxidation.

TABLE II

A Comparison of Weight Gain, Thickness of Oxides and Other Layers Measured by Microscopic and Microhardness Measurements

Alloy	Time (min)	Wt. gain/area (mg/cm^2)	Thickness of ThO_2+ZrO_2 cm x 10^{-2}	Thickness of ThO_2+Zr cm x 10^{-2}	Thickness of ThO_2+αZr cm x 10^{-2}	% change in thickness of sample
Zr-30 Th	1200°C 15	27	1.32	1.32	.41	8.6
	30	45	2.12	1.35	--	--
	60	55	2.61	3.59	.61	19.3
	120	72	4.24	5.56	1.12	29.2
	1400°C 5	60.5	3.10	2.54	.75	--
	10	67.3	3.56	2.96	.89	14.5
	10	38	3.44	1.67	.86	--
	15	99	5.80	3.12	.71	25.0
	25	110	4.05	2.30	.8	--
	30	128	6.8	>5.15	1.79	52.0
Zr-55 Th	1200°C 15	16	1.4	--	--	5.3
	30	23	1.65	1.4	--	--
	60	27.6	2.05	1.25	.53	5.4
	1400°C 10	37	2.75	1.41	.58	3.2
	20	43.1	3.68	1.70	.53	17.3
	25	48	3.18	1.4	.52	--
Zr-70 Th	1200°C 60	20.3	1.4	--	--	--
Zr-85 Th	1200°C 30	15.5	1.27	--	1.14	--
	60	20.3	1.57	--	.30	3.4
	120	29.2	2.7	--	1.65	8.3

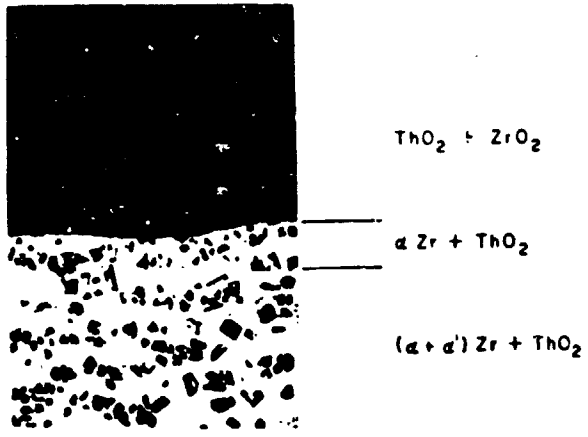

Zr - 30 % Th

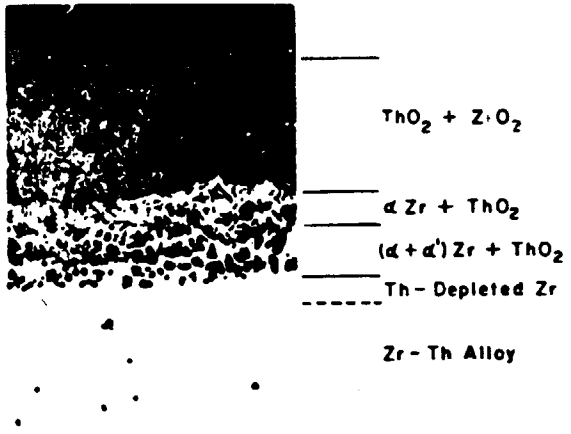

Zr - 55 % Th 20min

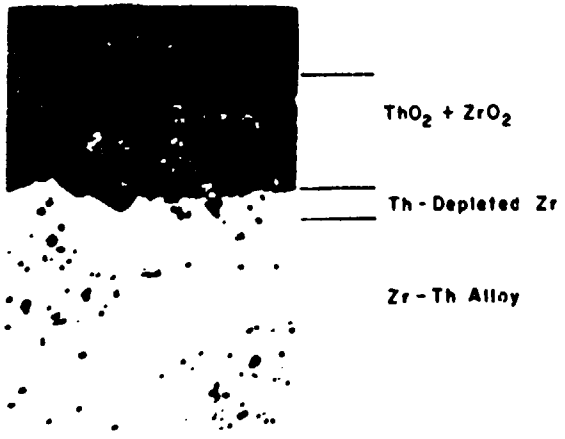

Zr - 55 % Th

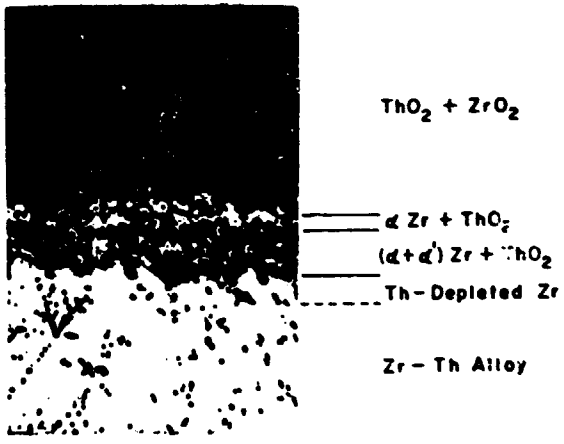

Zr - 55 % Th 25min

Hardness traverses of the single-phase metallic layer beneath the oxide were made on alloys oxidized at 1200 and 1400°C. The results given for the Zr-30%Th alloy in Fig. 7 are typical of the hardness traverses for the Zr-30%Th and Zr-55%Th alloys. The single-phase structure has a hardness above 1000 VHN near the oxide-metal interface, and in its entirety is harder than the substrate from which it is formed.

All of the layers thicken with time, and in the Zr-30%Th alloy, which was oxidized 30 minutes at 1400°C, the internally oxidized zone (layer 3) penetrated almost to the centerline of the specimen. In this sample large fissures in layer 2 and in the corners of the outer oxide layer were observed. The oxide was grossly distorted by growth, but cracks were observed only at corners and in the regions of the support hole in the specimen. In specimens oxidized at shorter times at 1400°C or equivalently shorter time at 1200°C, the corners were essentially intact and the external surface was sharply outlined as shown in Fig. 5 in Appendix I.

In the Zr-70%Th and Zr-85%Th alloys, the external oxide is the only layer which grows appreciably, and the rate of growth is considerably less than the rate in the thorium-lean alloys. Some indication of a small amount of internal oxidation at 1200°C may be present in the Zr-70%Th alloy structure shown in the previous report; however, internal oxidation and the solution of oxygen in the metallic matrix do not occur to an appreciable degree in the thorium-rich alloys. No single-phased region in the metallic matrix is observed, and hardnesses immediately adjacent to the metal-oxide interface indicate no hardening from oxygen solution.

At 1600°C observations were complicated by the fact that only the Zr-30%Th alloy was solid at temperature. In addition, the scales that formed on the liquid alloys were initially sound and nonporous but rapidly disintegrated at room temperature so that microstructure observations

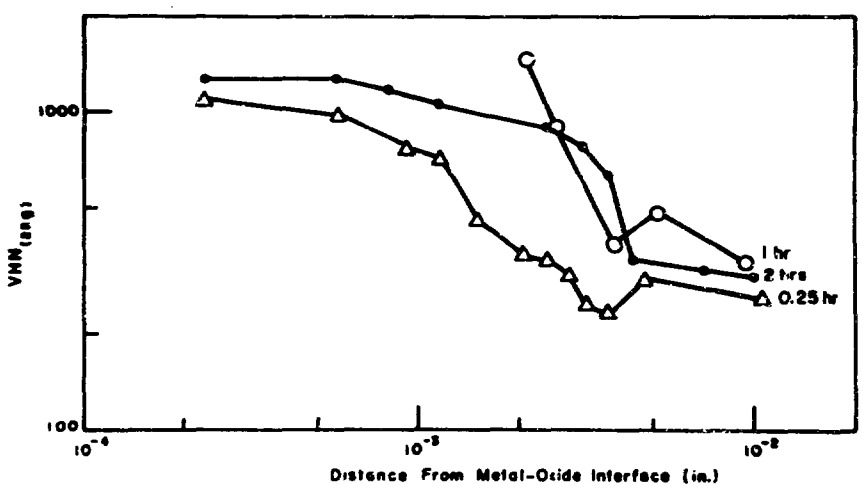

Fig. 7. The effect of oxidation time at 1200°C on the hardness of the metallic phase adjacent to the external oxide in Zr-30%Th specimens.

were not made. However, the disintegrated scales were analyzed by x-ray diffraction to determine their structure, and the following results were obtained:

Zr-55%Th:	ThO_2 + 10%ZrO_2 + (ZrN detected ≤ 5%)
Zr-70%Th:	ThO_2 + ≤ 5% (ZrN, (possibly ZrO_2) detected < 5%)
Zr-85%Th:	ThO_2 + ≤ 5% (ZrN + several unidentified lines – trace ZrO_2 ?)

The oxide that forms at 1600°C on the liquid alloys is predominantly ThO_2. The ZrO_2 observed in the Zr-55%Th alloy may have formed after the composition being oxidized was partially solid. These results indicate that thermodynamic considerations are overriding in the oxidation of the liquid alloys. Chemical analysis of the residual metal of Zr-55%Th samples oxidized for 15 and 30 minutes at 1600°C indicated thorium contents of 49 and 66.7% respectively. An alloy containing 45% thorium would be partly solid at 1600°C, and microscopic examination indicated localized areas where internal oxidation and an oxygen-saturated zone had formed, similar to that observed in the oxidation of the solid alloy.

2.3.3.2 Microprobe and X-ray Diffraction Studies

Microprobe analysis and x-ray diffraction studies of three alloys oxidized one-half hour at 1200°C have been completed during the current report period. The procedure used, the results, and a discussion of the results have been prepared by Battelle Memorial Institute and are included in Appendix A. In addition, preliminary x-ray diffraction studies of the Zr-30Th and Zr-85%Th alloys oxidized 2 hours at 1200°C and the Zr-30%Th alloy oxidized 20 minutes at 1400°C have been completed. These studies indicate that the sequence of phases observed at higher temperatures or longer times is essentially the same as that observed in the specimens oxidized 1/2 hour at 1200°C. Several conclusions can be drawn from the results of the microprobe and x-ray analysis which have

direct bearing on the rationalization of the oxidation processes at 1200 and 1400°C.

1. The external oxide scale formed on all samples is a two-phase structure of Th-rich and Zr-rich oxide. Although tetragonal ZrO_2 should be formed at high temperature, the tetragonal phase transforms to the monoclinic ZrO_2 on cooling and cubic ZrO_2 is observed as well.
2. In the Zr-85%Th alloy, the ZrO_2 structure is not observed by x-ray diffraction although the microprobe results indicate that considerable zirconium is present.
3. In the Zr-30Th and Zr-55%Th alloys, the internal oxide particles are largely ThO_2, but contain appreciable zirconium. The metallic matrix surrounding the particles is depleted in thorium.
4. In all samples, a metal diffusion gradient exists between the oxide affected substrate and the oxide scale or internally oxidized zone. This suggests diffusion of more reactive thorium into the oxide, and the diffusion of zirconium into the substrate as a result of the oxidation process.
5. In all cases, small amounts of zirconium nitride were found in the oxide scale formed.

By combining the microprobe, x-ray, metallographic and microhardness results, it is possible to describe the layers formed with greater accuracy, and even to assign approximate zirconium and thorium ratios of the phases observed. For example in the Zr-30%Th and Zr-55%Th alloys (14 a/o and 31 a/o Th respectively), the sequence of phases at 1200°C is as follows:

1. ZrO_2 (4 a/o Th) and ThO_2 (Zr content varies). Both cubic and monoclinic ZrO_2 are observed in the Zr-14 a/o Th alloy, although the tetragonal phase is stable at temperature. ZrN is present as a discrete phase in the oxide.
2. ThO_2 (~ 50 a/o Zr) + αZr (~ 2 a/o Th and up to 30 a/o O_2).
3. ThO_2 (~ 30 a/o Zr) + $\alpha + \beta Zr$ (~ 3 a/o Th).
4. A solid-solution zone in which the ratio of thorium to zirconium in the metal increases from 5 a/o and 14 a/o Th to the original alloy compositions of 14 and 31 a/o Th respectively.

In the Zr-85%Th (69 a/o Th) alloy, the sequence of layers or phases and the approximate composition is as follows:

1. A thin external two-phased oxide (ZrO_2 and ThO_2). The composition of the discrete phases is not defined.
2. A layer of ThO_2 (x-ray results indicate no ZrO_2 present) which contains 20 a/o Zr (x-ray results indicate some ZrN as a discrete phase, but the zirconium content in ThO_2 is uniformly high).
3. A metallic substrate in which the thorium content increases from ~ 20 a/o Th at the metal-oxide interface to the matrix composition (69 a/o Th).

The results of x-ray and microprobe tests now in progress will be used to check the accuracy of the quantitative values shown, as well as to provide information on the effect of time and temperature on the phases formed and composition of the phases.

2.3 DISCUSSION

2.3.1 Rate of Oxidation

The rates of oxidation at 1200, 1400 and 1600°C of the Zr-Th alloys are compared with previously determined rates of formation of ZrO_2 on liquid Zr-Sn alloys and ThO_2 on Th-Sn alloys in Fig. 8. At 1600°C, the parabolic rate constant for the alloys is located directly between the rate constants for the the oxidation of Zr and Th in Sn alloys. At 1200° and 1400°C the rates observed for the Zr-30Th and Zr-55Th alloys are considerably higher than a straightline average of the rates for Th and Zr in Sn. This suggests that the occurrence of internal oxidation is important in determining the overall rate constant for these alloys. The rate constants for the Zr-70%Th alloy at 1200 and 1400°C, and for the Zr-85%Th alloy at 1200°C are between the rate constants for the oxidation of pure Th and Zr. This indicates that the rates observed are an average of the rates determined by the diffusion of oxygen through the Zr and Th-rich two-phase oxide.

Internal oxidation eventually does lead to failure by breakaway in the Zr-30Th and Zr-55%Th alloys but the spalling occurs first in the oxygen-saturated Zr which leads to cracking of the oxide at the ends of the specimens. In the Zr-30%Th alloy, oxidized for 30 minutes at 1400°C, considerable spalling of the oxygen-saturated Zr had occurred cracks at the corners of the specimens; these cracks were apparently responsible for the increase in the rate of growth at longer times at 1400°C, and for shorter times at 1600°C. The most surprising fact is that the oxide does not spall in most of the alloys, even though the oxidation process causes a 10% or more increase in the thickness of the specimen. Even the corners of the specimen after 10% increase in thickness are essentially sound, with no indication of corner cracking in spite of the fact that the oxide is apparently being formed by anion diffusion at the metal oxide interface

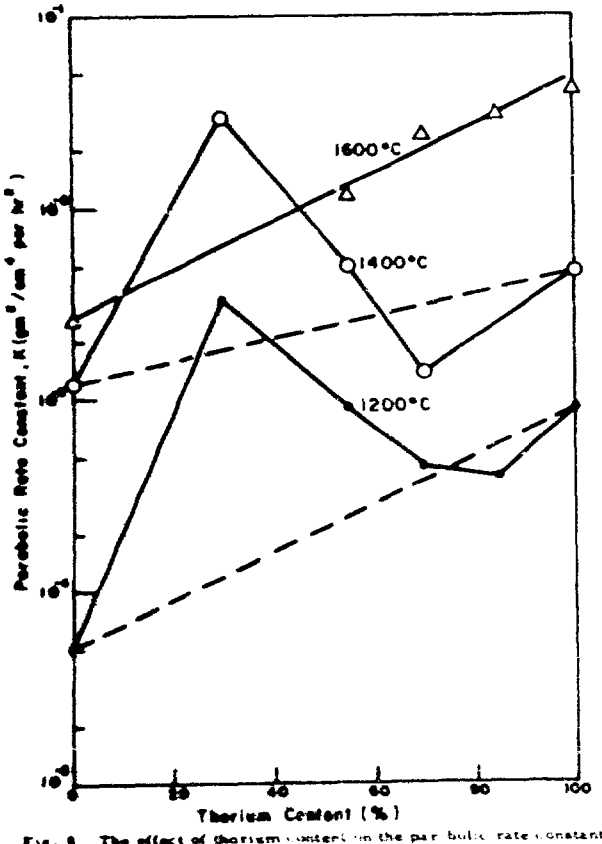

Fig. 8. The effect of thorium content on the parabolic rate constant in oxidation of Zr-Th alloys at 1200 to 1500°C. (Parabolic rates for Zr and Th obtained by interpolation or extrapolation.)

The fact that the oxide can undergo such distortion without cracking indicates that the two-phase structure of thoria surrounded by a mixture of zirconia or zirconia plus thoria-rich oxides, has considerable ductility at temperatures of 1200°C and above. If the growth of each layer observed after oxidation at 1200 to 1400°C is truly diffusion-controlled, then all layers should thicken with time, according to equation (1) where n = 1/2 and k is a different constant for each layer. The weight gain should be directly related to the rate of thickening of each zone and to the total thickness. In Fig. 9, the weight gain versus the thickness of the oxide layer, and the oxide layer plus internally oxidized zone is plotted for the Zr-30%Th alloy tested at 1200 and 1400°C. A linear relationship is obtained for both cases. Two conclusions are possible from these curves. First the thickness of the oxide layer for a given weight gain is independent of temperature, indicating that the oxide density (and probably composition) does not change with temperature. Second, the thickness of the internally oxidized zone does change with temperature, the layer being thicker for a given weight gain at 1200°C than at 1400°C. In the thorium-rich alloys, only the oxide layer grows with time, and the thickness of the oxide for a given weight gain is greater than that shown for the oxide layer in Fig. 9. This is not unexpected, since hardness and microstructure results indicate that almost all of the oxygen is in the oxide layer in the thorium-rich alloys.

2.3.2 Structure of Surface Zone

In order to discuss the sequence of phases at the air-coating interface in terms of the "ternary-diffusion" concept, it is first necessary to construct a tentative phase diagram for the Th-Zr-O ternary system. The Zr-Th and Zr-O binary diagrams are known and the quasibinary ZrO_2-ThO_2 diagram is also known. The Th-O diagram is not known, but the existence of oxide particles in a melted button containing 1500 ppm O_2 suggests that the solubility of oxygen in thorium is extremely low.

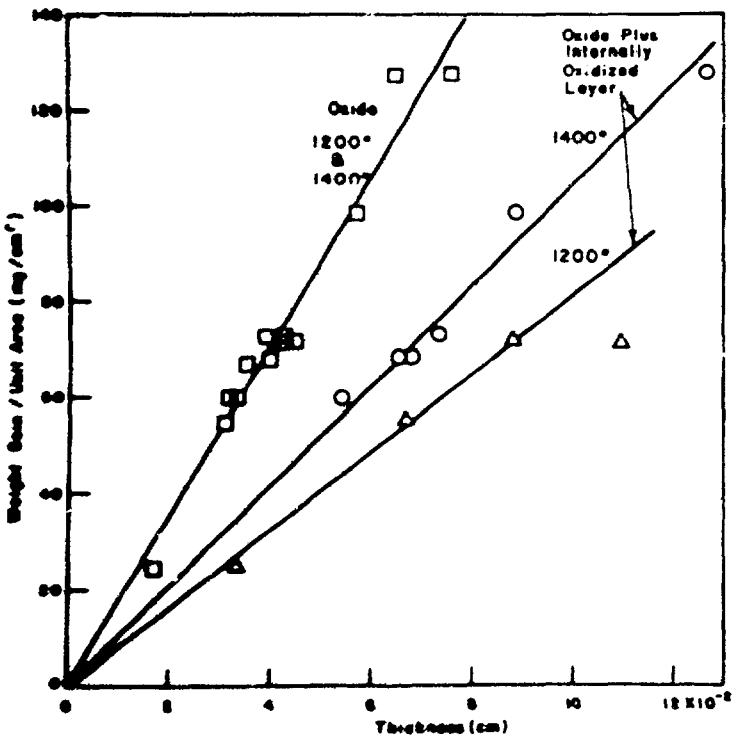

Fig. 9. Comparison of weight gain with oxide thickness and total oxide + internal oxidized layer for a Zr-30%Th alloy oxidized at 1200 and 1400°C.

The metallographic, hardness, x-ray diffraction and microprobe results of alloys oxidized at 1200°C define the zirconium-thorium ratio of the phases observed, the structure at temperature or structures which result from transformation on cooling, and permit an estimate of the oxygen gradient in the substrate. These results have been used to construct the tentative 1200° isotherm shown in Fig. 10. The cubic zirconia found in the oxide of the Zr-30%Th alloy has not been included in this diagram since Roy and Mumpton[1] have shown that the cubic zirconia observed in ThO_2-ZrO_2 alloys is a metastable rather than stable phase.

It is not known whether the metastable phase is formed at temperature or on cooling, but a three-phased region should not be observed unless one of the phases is metastable. The low solubility of thorium (< 2 a/o) in the oxygen-rich internally oxidized zone of the Zr-14 a/o Th and Zr-31 a/o Th alloys helps to establish the oxygen gradient since the oxygen content of the zirconium-oxygen phases at the limit of solubility of thorium in these phases should not differ greatly from that in the Zr-O binary diagram. The low thorium content between the substrate and the internally-oxidized interface, and the identification of the internal oxide as ThO_2 suggests that the $\beta + ThO_2$ two-phase region exists at very low thorium and oxygen contents. Finally, the high zirconium contents of the ThO_2 in the $\alpha + ThO_2$ and $\beta + ThO_2$ internally oxidized layers in the thorium-lean alloys was used to construct the extended ThO_2 single-phase region with the assumption that this region is qualitatively only slightly oxygen-lean. The three-phase regions were observed as boundaries between layers. The $\alpha_2 + \beta + ThO_2$ and $\alpha_2 + ThO_2$ regions were not encountered in the diffusion couples but must exist at 1200°C.

The tentative diffusion paths of the Zr-14 a/o Th, Zr-31 a/o Th and Zr-60 a/o Th alloys at 1200°C are also indicated in Fig. 10. In the

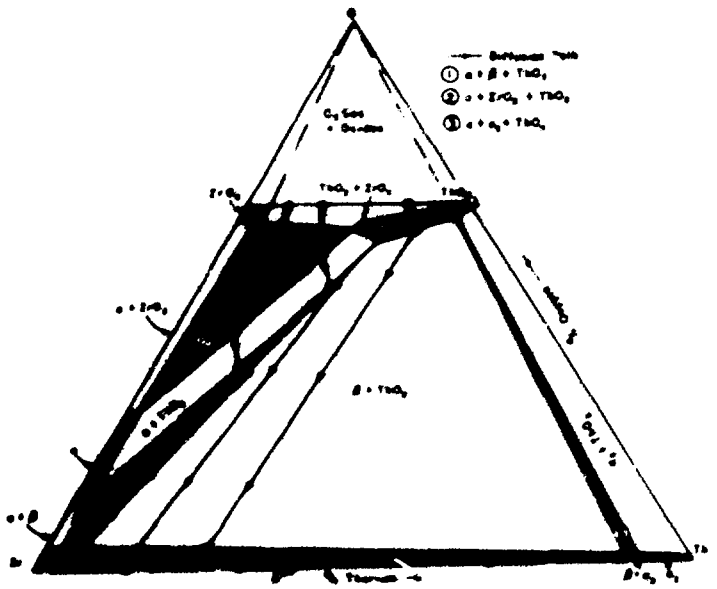

Fig. 16. Tentative phase diagram at 1200°C of Th-Zr-O system based on microprobe, x-ray and microstructure observations in oxidation of three Zr-Th alloys. Composition paths for oxidation of 3 Zr-Th alloys are indicated by arrowed lines.

Zr-14 a/o Th and Zr-31 a/o Th alloys the composition paths crosses tie lines in the ThO_2 + ZrC , α Zr + ThO_2 and β + ThO_2 two-phase regions, and thus the internally oxidized layers as well as the two-phased oxide layer is observed in the microstructure. A net material flow of thorium from the unaltered substrate to form the thorium-lean metallic zone and oxide phases richer in thorium is apparent in all alloys.

In the Zr-69 a/o Th alloy the composition path through the β + ThO_2 region is also a tie line so that the two-phase region is observed as a boundary between the oxide and substrate rather than an internally oxidized zone. The external layer of the oxide is two-phased ThO_2 and ZrO_2 since tie lines are crossed. The existence of a single-phase zirconium-rich ThO_2 solid solution agrees with the microstructure and the microprobe results. Although ZrO_2 is observed by x-ray diffraction only in the outer portion of the scale, the presence of large amounts of zirconium in the oxide formed indicates that a layer of single-phase oxide exists in the oxidized specimen.

Nitrogen has been ignored in the analysis of the specimens even though zirconium nitride has been detected in the oxide scales formed. The amount of nitride formed is small and the overall reaction does not seem to involve nitrogen to an appreciable extent. However, in order to check this point, a limited number of samples will be oxidized in an argon-oxygen mixture.

The diffusion paths and phase diagram in Fig. 16 are reasonably consistent, and speculation on the kinetics of diffusion in certain cases is possible. In the Zr-14 to 31 a/o Th alloys, the flux of thorium to the metal-oxide interface is not sufficient to combine with all of the oxygen, and as a net result, oxygen diffuses into the thorium-depleted metallic substrate until the solubility limit is reached for a given thorium-zirconium

ratio. Thorium oxide nucleates and grows as an internal oxide until the faster diffusing oxygen consumes the thorium available locally and diffuses into the substrate to nucleate additional ThO_2-rich particles at a point further removed from the surface of the specimen.

If this process is active in the Zr-30 to 55%Th alloys, the ratio of the diffusion of oxygen to the diffusion of thorium must decrease with increasing temperature, since the particles nucleate with greater frequency at the higher temperatures. The spatial density of internally oxidised particles in the substrate is greater at higher temperature, and the thickness of the internally oxidised boundary in relation to the thickness of the external oxide decreases with increasing temperature.

A report of the oxidation of Cb-Zr alloys, by Speisser and Gordon,[2] also indicated that oxidation of alloys containing approximately 50 a/o Zr occurs by a process involving internal oxidation. However, in contrast to the internal oxide observed in the thorium-zirconium system, the internal oxide formed in the zirconium-columbium system is a continuous zirconium-rich oxide which forms from the alpha zirconium platelets. These results indicate that the morphology of the internally oxidised particles depends to some extent on the solubility of oxygen in the more reactive metal. In the Zr-Cb alloys, solution of oxygen in the matrix causes the formation of alpha zirconium platelets which oxidise at a more rapid rate and in preference to Cb-rich beta; as a result a continuous network of internal oxide is formed.

The most surprising result is that oxidation at 1200 to 1400°C occurs without breakaway even though stress is generated during oxidation. The corners of the specimens retain a sharp 90° angle, even after the oxide formed causes an increase in thickness of 10% or more. These results indicate that the oxide can accommodate large strains at 1200 to 1400°C without cracking, and thus prevent breakaway or spalling of the

oxide which would lead to linear oxidation.

The non-protective growth of oxides over the alloys at 1000°C and 750°C can now be rationalized if the strains which must be accommodated at the metal-oxide interface during the growth of the oxide are considered. The spalling of the oxide at 750 and 1000°C seems to be the direct result of poor ductility in the two-phase oxides at these temperatures. The strains due to growth at the metal-oxide interface cause high shear and tensile stresses in the oxide which cause fracture at 750 and 1000°C but apparently cause deformation without cracking in the two-phase oxide at higher temperatures.

2.4 CONCLUSIONS

The results of our work to date on the oxidation of Zr-Th alloys have led to the following conclusions:

1. Oxidation at temperatures from 750 to 1000°C is linear due to the spalling of the oxide formed, which results from the generation of mechanical stresses during the growth of the oxide.
2. Oxidation at 1200°C to 1400°C is diffusion-controlled, and the films formed are compact and adherent.
3. Oxides formed at 1200°C and above accommodate thickness increases of 10% or more without cracking or breakaway oxidation.
4. The rates of diffusion-controlled oxidation are considerably higher for alloys that form internally oxidized zones than for alloys that do not.

5. Insofar as the limited data on diffusion paths and phase diagram are valid:
   a. the composition paths in the ternary phase diagram do not cross,
   b. two-phased structures are observed when tie lines are crossed, but not when the diffusion path follows a tie line.
   c. the morphology and existence of a two-phased internally oxidized zone depend upon the relative diffusion rates of the metals and oxygen, as well as the phase equilibria (e.g., solubilities in the Th-Zr-O in contrast to the Cb-Zr-O systems).

2.5 FUTURE WORK

The additional microprobe and x-ray results, and oxidation of two alloys at 1200°C in an argon-oxygen atmosphere, will be completed during the next report period.

3. THE ThN-ZrN-O SYSTEM

3.1 EXPERIMENTAL PROCEDURE

The study of the ThN-ZrN-O system has both fundamental and applied significance. Some Th-Zr alloys are liquid at temperatures of 1420°C and above, while the nitrides are not. Similarly, the phases observed and crystal structure of the phases in the ThN-ZrN and Th-Zr systems differ quite drastically. The knowledge to be gained by study of this system is an insight into the effect of substrate state or crystal structure, morphology and properties on the tendency toward breakaway. This system has a practical objective as well, since nitrides of tungsten are unstable and many refractory nitrides do not react with tungsten at 2800°C. Also, the nitrides (and carbides) of many metals that form refractory oxides

are quite refractory -- a desirable property in a reservoir coating layer. Thus the system represents a type which could be of particular significance to the protection of tungsten.

Coupons of the four Zr-Th alloys were cut from the sheet used in the study of oxidation of these alloys. The coupons were nitrided in dry nitrogen at 1300°C for 6 hours, and specimens were oxidized at 1150, 1200, and 1600°C. Measurements of the weight gains during the nitriding and oxidation tests were made, and microstructures of the nitrided specimens and of samples oxidized at 1200 and 1600°C have been examined metallographically. Microhardness traverses of several oxidized specimens have been made.

3.2 RESULTS

The weight gains during nitriding of the Zr-30, 55, 70 and 85% Th alloys, together with thickness measurements of the nitride formed on the Zr-30%Th and Zr-55%Th alloys, are given in Table III. The rate of nitrogen pick-up is very composition-dependent. For example, the amount picked up in 6 hours at 1300°C was only 1.08 to 1.8 mg/cm^2 for the Zr-30%Th alloy, but was 21 to 50 mg/cm^2 for the Zr-85%Th alloy. Structures typical of nitrided specimens are shown in Fig. 11 for three alloys. In the Zr-30%Th alloy, an external single-phase layer, probably ZrN, is formed at the surface. A similar layer is observed in the Zr-55% Th alloy; however, in this sample, a subscale layer which may be α-Zr saturated with nitrogen is also observed. In the Zr-85%Th alloy, the nitride is two-phased, consisting of a grey matrix, probably a thorium-rich nitride and angular Widemanstatten particles which have the typical gold color of ZrN. Thus, the increased nitriding rate in the 70 and 85%Th alloys is associated with the formation of a matrix of thorium-rich nitride. Samples of nitrided Zr-70%Th and Zr-85%Th decompose readily in air.

TABLE III

Oxidation of Partially Nitrided Zr-Th Coupons at Several Temperatures

Composition	Nitrided 1300°C, 6 hrs		Oxidation						Remarks
	Wt. gain (mg/cm^2)	Thickness nitride (cm)	Temp. (°C)	Time (hr)	Wt. gain (mg/cm^2)	Oxide (cm)	Internal layer (cm)	Saturated layer (cm)	
Zr-30 Th	1.48	0.0004							
	1.77	--	1150	0.25	29	--	--	--	White
				0.5	35				
				0.75	39				
	1.08	--	1200	0.09	33				
				0.17	56				
	1.80	--	1200	0.17	--	0.020	0.014	0.003	Micro-probe
	1.78	--	1600	0.17	87	0.044	0.044	--	
Zr-55 Th	5.57	0.0007 & 0.00164(2)	1150	0.25	51.4				
	5.1								
	5.15		1200	0.09	35				
				0.17	59				
	3.7		1200	0.17	--	0.036			
	3.7		1600	0.17	46	0.038	0.030	--	Spalled
Zr-70 Th	26.1		1150	0.25	21.5				
Zr-85 Th	21.4(1)		--						
	54.1(1)		1150	0.25	11				
	47.9(1)		1200	0.09	8.9				
				0.17	14.0				
	22.1(1)		1200	0.17		0.026	0.008		Oxide decomposes
	51.1(1)		1600	0.17	21.2	0.015	0.046		

(1) Samples blistered.
(2) Two zones in microstructur .

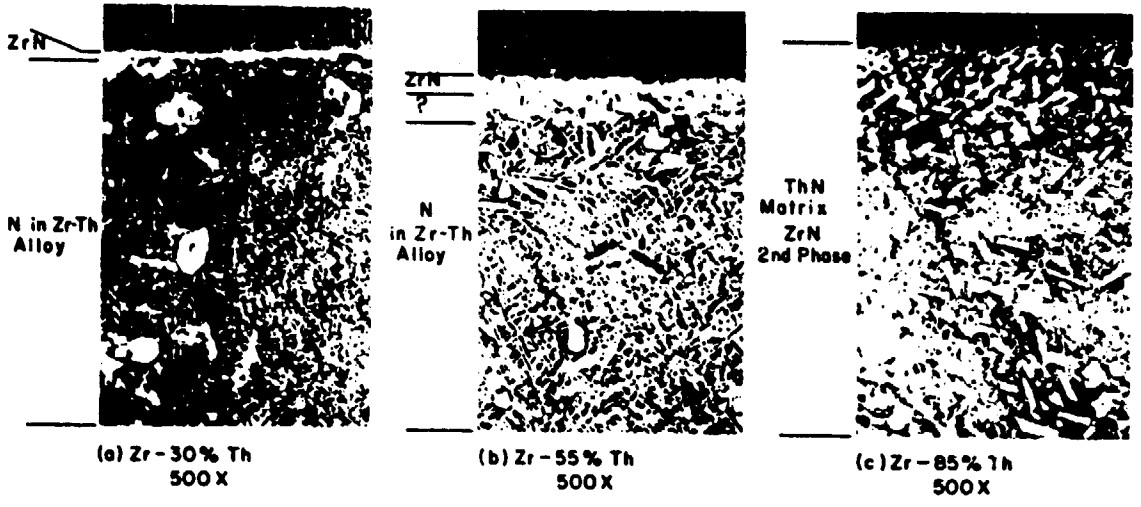

Fig. 11. Structure of layers formed in Zr-Th alloys nitrided 6 hours at 1300°C.

and the structure observed in the microscope changes drastically within 5 minutes.

Oxidation of the partially nitrided specimens at 1150 and 1200°C occurs quite rapidly, as shown in Table III, and the structures observed in the Zr-30%Th and Zr-55%Th alloys are quite similar to that observed in the oxidation at 1200°C of the unnitrided alloys of the same composition. Hardness traverses indicate an oxygen or nitrogen-saturated α-Zr layer immediately adjacent to the external oxide, and particles which may be nitride are also observed in the oxide layer.

In the Zr-85%Th alloy, the structure is quite different from that produced in oxidation of the unnitrided alloy, as shown in Fig. 12a. In the nitrided speciment, a porous layer of mixed oxides is formed which is apparently nonprotective, and a subscale layer, apparently ThO_2 and ZrN, is also observed.

Oxidation proceeds rapidly at 1600°C and the oxides formed after 10 minutes are 0.06 to 0.09 cm thick. The structures of layers observed after oxidation at 1600°C (Figs. 12b and 12c) are quite different from those observed after oxidation at 1200°C. In the nitrided Zr-85%Th alloy, the outer layer of mixed oxides is not badly spalled and this layer seems to be coherent with the layer which contains ThO_2 plus residual ZrN. Oxidation proceeds quite readily in the thorium-rich nitride matrix, but apparently ZrN reacts more slowly with oxygen.

The scale formed at 1600°C on the nitrided Zr-55%Th alloy is also two-phased, but in the oxidation of the nitrided alloy, the continuous phase is the darker ThO_2, so that internal oxidation occurs by diffusion through a continuous ThO_2 phase, and oxidation of the Zr saturated with oxygen or nitrogen does not occur readily.

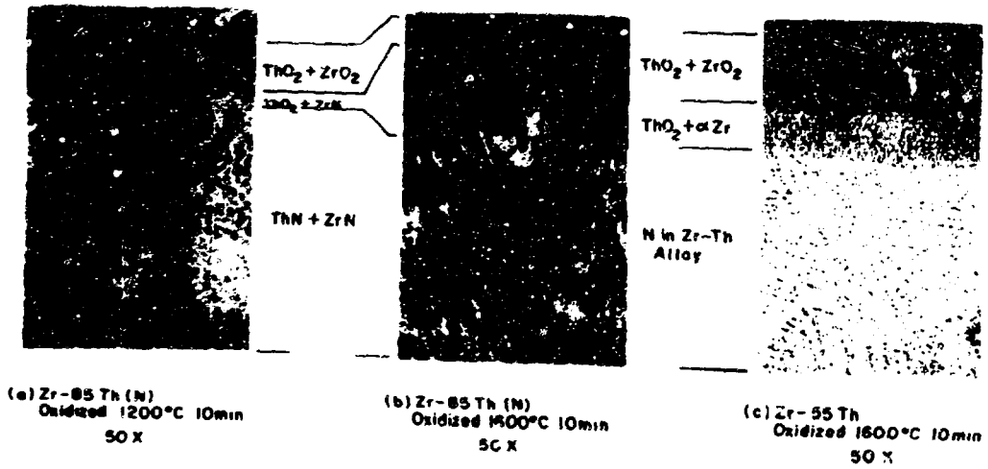

Fig. 12. Layers formed during the oxidation of nitrided Zr-Th alloy oxidized at 1200 and 1500°C.

The oxide formed on the Zr-70%Th and Zr-85%Th alloy also decomposed or disintegrated to a fine powder on standing, even in a desiccator.

3.3 DISCUSSION OF RESULTS

The effect of composition on the rate of nitriding can be rationalized in terms of the structures observed. The nitride formed on the Zr-30%Th and the Zr-55%Th alloys has the characteristic gold color of ZrN, and apparently diffusion of nitrogen through ZrN occurs at a very slow rate. The formation of a two-phase nitride on the Zr-70%Th and Zr-85%Th alloys suggests that there is a two-phase region in the ZrN-ThN quasi-binary phase diagram. The matrix phase in the latter alloys is apparently a thorium-rich nitride, and the fact that the nitriding rate is more rapid indicates a more rapid diffusion rate of nitrogen in thorium nitride. The tendency for the nitrides of these alloys to decompose in air is also characteristic of thorium nitrides.

Since the Zr-30%Th and the Zr-55%Th alloys were only partially nitrided, analysis of the oxidation behavior of the specimens will not be attempted. Even in the Zr-70%Th and Zr-85%Th alloys (which were nitrided completely) the behavior must be inferred from structure and weight gain observations, since only one sample was oxidized at each temperature. At 1200°C, the oxide formed (Fig. 12) is porous and badly spalled; the thickness of the oxide is greater than observed on the unnitrided alloy, and a zone of internal oxidation is observed. Thickness and microstructure evidence suggest rapid linear oxidation. The oxide and oxide plus nitride layers formed at 1600°C appear to be sound, and the thickness after 10 minutes is not unreasonable for 10 minutes at 1600°C.

The oxides formed at 1150 to 1600°C on the nitrided Zr-70%Th and Zr-85%Th alloys disintegrated or reacted at room temperature to form a fine powder, similar to that formed on the 1600°C liquid Zr-Th metal alloys.

The formation of an internally oxidized zone, which bypasses the gold ZrN phase in the nitride, suggests that diffusion of oxygen through the thorium-rich oxide occurs rapidly. However, the dense scale formed at 1600°C indicates that the nitrogen evolved escapes by diffusion, rather than eruption, in the thorium-rich alloys. Thus, it is possible to evolve a gas without causing breakaway.

These observations, and the tendency for the thorium-rich oxides to powder, suggest that further work with nitrided thorium-zirconium alloys, or similar alloys, be conducted on alloys containing less than 70% thorium. Additional alloys will be prepared in the range of Zr-5%Th to Zr-60%Th, in the form of rod specimens, rather than sheet. The procedure for nitriding rods of 3/16 in diameter has been worked out using Hf and Zr wire. Future experiments of oxidation in the Zr-Th-N system will utilize specimens nitrided in this manner.

4. THE W-Hf-O SYSTEM

The W-Hf-O system is one of special interest to the oxidation protection of tungsten at very high temperatures because of the refractory nature of HfO_2 and the existence in the W-Hf binary system of a very refractory compound, W_2Hf, which could form the basis of a protective coating system. Therefore, a study is being made of the oxidation of W-Hf alloys to gain some insight into the types and morphology of the oxide layers formed and their relationship to thermodynamic and kinetic factors in this system.

4.1 EXPERIMENTAL PROCEDURE

During the current report period, additional tungsten alloys containing 2, 19, 69, and 95%Hf have been produced by arc melting, as previously described. With the exception of W-69%Hf, the alloys could be fabricated to sheet for preparation of coupon test specimens. Specimens were oxidized for several times at temperatures of from 1000 to 1600°C, and the change in weight during oxidation was measured. In addition, the rate of recession of the metal interface was measured on sections of specimens mounted and prepared for microscopic examination. On specimens not prepared for microscopic examination, the oxide was removed by light sand-blasting and the thickness of remaining metal was measured directly. Chemical and x-ray diffraction analyses of the W-32.5%Hf and W-34.9%Hf alloys were made on the original alloys and on the oxide formed during oxidation.

4.2 RESULTS

The weight gain in one hour and the metal recession after one hour was determined by interpolation or extrapolation of a log-log plot of weight gain or recession versus time, and the results are given in Table IV. The type of growth is also indicated in Table IV, either as parabolic or linear, from the slope of the recession or weight gain time curves. In alloys where accurate measurements of the area were possible, the rate constant is also indicated.

Two-phased structures were observed in all alloys except the W-2%Hf alloy, even though the phase diagram indicates that the W-32.5%Hf and W-34.2%Hf alloy should be single-phase. Results of chemical and x-ray diffraction analyses and the hafnium content of the oxides formed on the two alloys is given in Table V.

TABLE IV

A Comparison of Weight Gains with Metal Gains with Metal Recession of W-Hf Alloys Oxidized in Air at Various Temperatures

Alloy	Temp. (°C)	Wt. gain in 1 hr. (mg/cm^2)	Type of growth	Color of oxide	Metal recession in 1 hr. ($cm \times 10^{-3}$)	Rate K_p (mg^2/cm^4 per hr)
W-2% Hf	1000	12.5	p	Gray-Black	1.3	1.50×10^{-4}
	1300	82.0	p	Black	20.0	6.7×10^{-3}
	1600	70.0	l*	Black	140.0	
W-19% Hf	1000	15.0	~p	Yellow-Black	6.0	
	1300	26.0	p	Gray-White	36	
	1600	37.0	l*	Yellow-Black	270	
W-32.5% Hf	1000	--	l (cyclic)	Yellow	13.5	
	1000	--	l	Yellow	12	
	1300	--	l (cyclic)	Yellow-White	13.0	
	1300	--	l	Yellow	6.3	
	1400	Evap.		Yellow		
	1600	Evap.	~l	Yellow-White	80	
W-34.2% Hf	1000	--	~l	White	10.3	
	1300	58	p	White	20.0	3.4×10^{-3}
	1300		l	Yellow	25.4	
	1400	Evap.		Yellow	36.8	
W-69% Hf	1000	120	~l	Yellow	40	
	1300	92	~p	White	21.5	8.45×10^{-3}
	1600	Evap.	p		44	
W-95% Hf	1000	8	p	White	2.0	6.4×10^{-5}
	1300	45	l	White	20.0	
	1600	Weight loss	l	Black	15.0	

p - Parabolic from weight gain.
l - Linear weight gain.
* - From recession.

TABLE V

Microscopic, Chemical and X-ray Analyses of Alloys and Oxidation Products in W-32.5 Hf and W-34.2 Hf Alloy

	Analysis
W-32.5 Hf Alloy	
Alloy composition	32.5% Hf
Structures (x-ray diffraction)	$W_2Hf + Hf_{ss} + W_{ss}$
External oxide (1 hr. 1300°C)	59.9% Hf (32% W)*
External oxide (1 hr. 1600°C)	25.8% Hf (5.5% W)*
Sample (1 hr. 1600°C)	Thickness of:
	black subscale 2.4×10^{-6} cm
	mixed subscale 3.3×10^{-3} cm
W-34.2 Hf Alloy	
Alloy composition	34.9% Hf
Structures (x-ray diffraction)	$W_2Hf + W_{ss} + Hf_{ss}$ (2 strong unidentified lines)
External oxide (1 hr. at 1600°C)	21.8 Hf (58.5 W)* W-rich
External oxide (1 hr. at 1600°C)	Thickness of:
	black subscale 3.3×10^{-3} cm
	mixed subscale 2.5×10^{-3} cm

* Assumes WO_3 and estimated by ternary diagram on WO_3-HfO_2 line.

The structures observed in oxidation of the two-phase alloys are both composition- and temperature-dependent, as shown by the results for the W-19%Hf alloy oxidized at 1300 and 1600°C (Fig. 13), and the W-69%Hf alloy oxidized at 1000 and 1300°C (Fig. 14). At 1300°C, the oxide on both alloys formed at a rate which was approximately parabolic. The oxide on the W-69%Hf alloy at 1000°C formed rapidly at the metal-oxide interface. The corners and edges were deeply grooved, which resulted in a cruciform appearance after oxidation. At 1600°C, vaporization occurred in the oxidation of all compositions, as indicated by an initial gain in weight, followed by a decrease in a total weight gain at longer times for most alloys. The rates of metal recession, rather than the changes in weight, were used to determine the kinetics of oxidation.

4.3 DISCUSSION

The effect of composition on the rate of oxidation depends on the temperature at which oxidation occurs in the W-Hf system, Fig. 15. At 1000°C, the single-phased terminal compositions oxidized at a rate which is much less than that shown for the two-phase alloy. However, at 1300°C and above, the intermediate alloys which contained tungsten-hafnide or tungsten-hafnide plus excess hafnium recess at a slower rate. Examination of the microstructure of the W-69%Hf alloy (Fig. 16b) indicates that a single phase layer is formed at the metal oxide interface which is probably the intermetallic compound W_2Hf. Unfortunately, the two alloys which should have been single phased (32.5 and 34.9%Hf) were not homogeneous, as indicated by the microstructures and the fact that both W-rich and Hf-rich phases were identified in addition to W_2Hf. In sections tested at 1000°C, internally oxidized zones of both alloys were observed, which suggests preferential oxidation of one of the phases present.

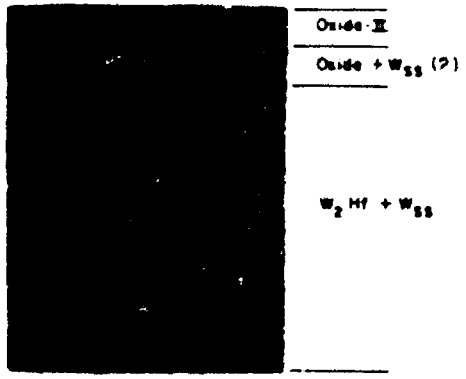

Oxidized 1800°C .086 hr
100 X

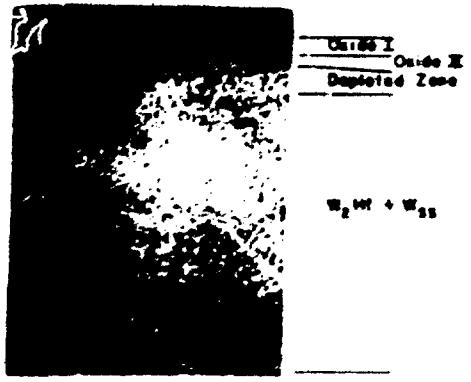

Oxidized 1300°C 2.25 hrs
100 X

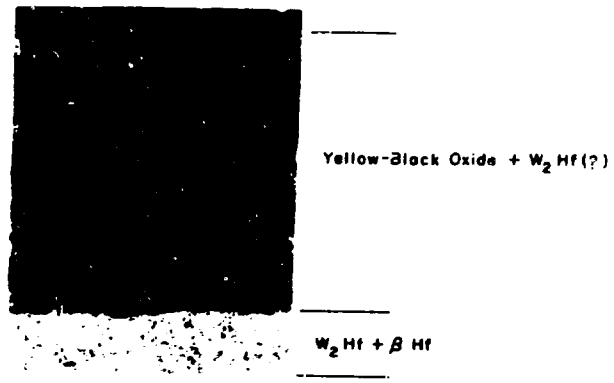

(a) Oxidized 1000°C – .75 hr
50 X

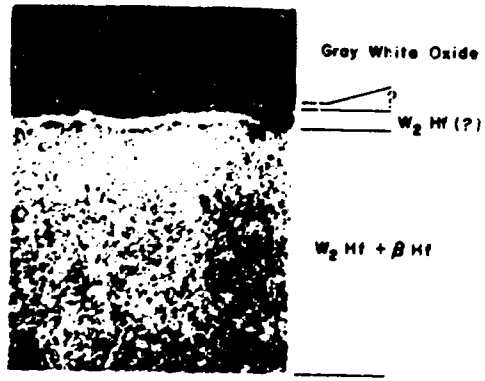

(b) Oxidized 1300°C – .5 hr
50 X

Fig. 14. The effect of temperature on the oxidation of the W-69%Hf alloy (two phased W_2Hf + Hf_{ss}).

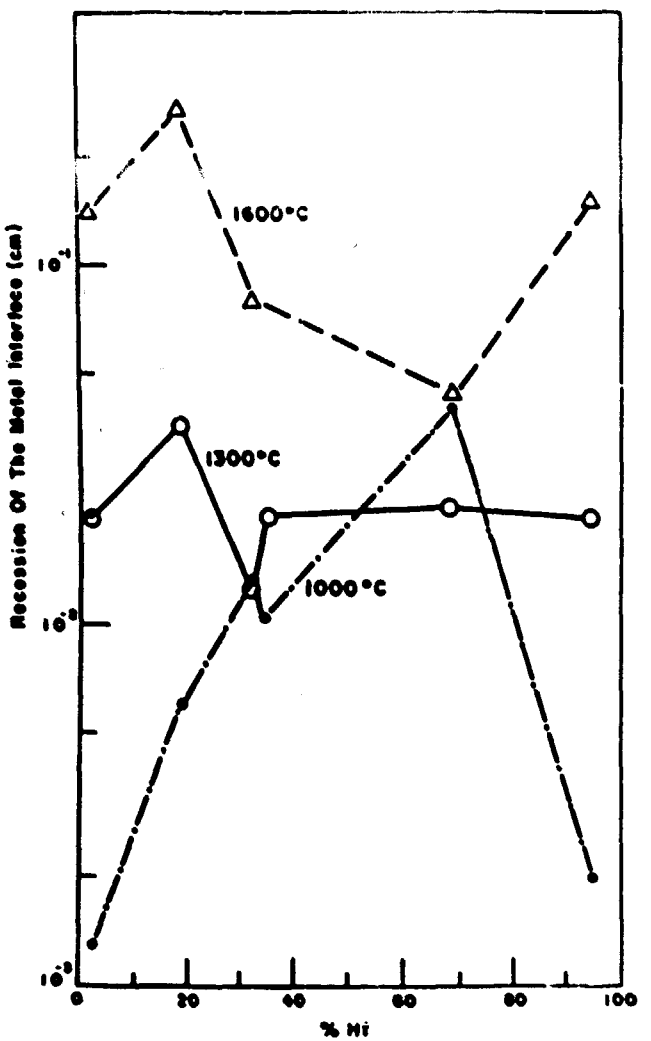

Fig. 19. The effect of composition and temperature on the metal thickness consumed in oxidation of W-Hf alloys for one hour.

The sharp contrast between the effect of temperature on two-phased W-1.9%Hf alloy and the two-phased hafnium-rich W-6.7% alloy is interesting. In the W-1.9%Hf alloy, the two phases present should be the tungsten solid solution and tungsten-hafnium compound. In this alloy, internal oxidation was observed only at 1600°C. In the W-6.7%Hf alloy, however, internal oxidation of the hafnium-rich phase probably occurred only at 1000°C. Oxidation at 1600°C proceeded by diffusion through a single-phase region which is probably W_2Hf, and the rate of growth was considerably lower.

4.0 FUTURE WORK

During the next report period, efforts will be devoted to determining the oxidation behavior of single-phased W_2Hf. Samples of W_2Hf will be prepared by passing a molten zone along a bar of suitable composition in an electron-beam zone refiner and annealing at a very high temperature to insure the formation of a single phase. The ternary Mo-Hf-Re phase diagram has recently been reported,[3] which shows a compound $(Mo,Re.)_2Hf$ exists as a single phase region with a much wider range of Hf concentration. The similarity between the compounds, Mo_2Hf and W_2Hf suggest that the W-Re-Hf ternary phase diagram should be similar. Preliminary melts of compositions which should form Hf-rich and Hf-lean intermetallic compound will be prepared and examined microstructurally to determine whether the addition of Re to the W_2Hf will permit the study of the wider range of Hf concentrations.

5. Al-Sn-Cr SYSTEM

In previous experimental work on refractory oxides, it was demonstrated that breakaway could be prevented by the use of liquid substrates. This work also showed that the growth rate during oxidation of

pure refractory oxides was greater than could be tolerated.[4] The basic factors affecting the diffusion rate in oxides at very high temperatures are relatively unexplored. Information on the diffusion rate of O_{18} in pure alumina[5] at temperatures up to 1775°C indicated that impurities have a marked effect on the diffusion rate at lower temperatures but that at temperatures of 1600°C and above, the diffusion rate is more dependent on thermally activated vacancies than any other factor. Hensler and Henry[6] have demonstrated that the addition of 1% Cr_2O_3 to Al_2O_3 causes a substantial increase in the resistivity at 1000°C to 1400°C, and a similar peak in resistivity at 95% Cr_2O_3 is observed. Since both chromium and aluminum exist primarily at a valence of +3, and Cr_2O_3 and Al_2O_3 form a continuous solid solution with a corundum crystal structure, it is difficult to explain these results on the basis of Wagner's theories. Therefore, in the current report period oxidation studies of liquid Sn-Al Cr alloys were started to determine if it is possible to grow a mixed aluminum-chromium oxide from such a liquid substrate, to determine the growth characteristics of this oxide, and to see if the rates of growth of the mixed oxide was lower than that of pure Al_2O_3 grown from liquid Sn-Al alloys.

5.1 PROCEDURE AND RESULTS

Alloys containing 5%Al and approximately 95%Sn with additions of 0.05, 0.1, 0.25 and 0.5%Cr were melted in zirconia crucibles in an inert atmosphere at 1350°C and subsequently oxidized at 1300 and 1600°C. Additional melts of 95%Sn-5%Al were oxidized at 1600°C for comparison. The ratio of aluminum to chromium in the liquid alloys was from 100-1 to 10-1. Microstructures of some of the oxidized alloys were examined, and the thickness of the oxide formed was measured. In addition, selected chemical analyses were made for control purposes.

The results of oxidation tests at 1300 and 1600°C are given in Table VI for tests run without interruption for the periods shown and for tests cooled intermittently to room temperature to measure the weight gain at various times during the test interim. In those tests where cycling oxidation was used, a change from parabolic to a partially linear growth rate occurred in some samples to which chromium additions had been made. The chromium content of the oxide formed on the 95Sn-5Al-.05Cr alloy was determined to be 0.12%Cr, the remainder of the oxide being Al_2O_3. Additional tests of a residue that formed on the furnace during melting indicated that chromium, aluminum and tin are contained in the residue, and that chromium was not present in amounts greater than in the liquid alloy.

5.2 DISCUSSION OF RESULTS

Although it would be premature to draw any conclusions from the data obtained to date on the Al-Sn-Cr-O system, the addition of small amounts of chromium does seem to influence the oxidation rate at 1600°C, as shown in Fig. 16. A minimum in the weight gain after 8 and 16 hours at 1600°C seems to occur at a 0.05 to 0.1% chromium addition in the liquid metal. Chemical analysis indicates that the chromium content of the Al_2O_3 formed in the protective layer is approximately 0.1%. Although these results are not in complete agreement with the composition at which maximum resistance was observed in the Al_2O_3-Zr_2O_3 alloys by Hensler, the minimum chromium content studied in the electrical resistivity experiments was 1% Cr_2O_3.

TABLE VI

The Effect of Cr Additions on the Rate of Oxidation of Al-Sn Liquid Alloys

Alloy	Temp (°C)	Time (hrs)	W/A (mg/cm²)	Oxide increase (mils)	Remarks
95 Sn-5 Al	1300	0	2.5		
	1300	8*	8.2		n = 1/2
	1300	16*	10.7		n = 1/2
	1600	0	21.0		
	1600	0	25.0	0.7	
	1600	0	27.9	0.95	
	1600	0	56.0		
	1600	8*	30.0		n = 1/2
	1600	16*	40.0		n = 1/2
95 Sn-5 Al + 0.05% Cr	1300	0	1.5		
	1300	8*	8.2		n = 1/3.3*
	1300	16*	9.9		n = 1/3.3*
	1600	0	11.1	0.8	Internal oxide particles
	1600	16	31.2	0.9	Internal oxide particles
95 Sn-5 Al + 0.1% Cr	1300	0	2.6		
	1300	8*	2.9		Partially linear values indicated
	1300	16*	6.4		
	1600	0	20.4	1.5	Internal oxide particles
		16	33.0	1.0	
95 Sn-5 Al + 0.19% Cr	1300	0	3.9		
	1300	8*	5.0		Partially linear (9.0)
	1300	16*	7.0		Partially linear (12.3)
	1600	0	30.0	1.1	
	1600	16	140.0	1.5	
95 Sn-5 Al + 0.59% Cr	1300	0	3.7		
	1300	8*	2.7		Partially linear (5.0)
	1300	16*	6.0		Partially linear (14.0)
	1600	0	60.6	0.95	
		16	62.0	1.5	

* Cyclic tests with intermediate weight measurements

W/A obtained by extrapolation from log-log plot of W/A vs time from portion where exhibits a slope of 1/2. Actual value of W/A is indicated in remarks

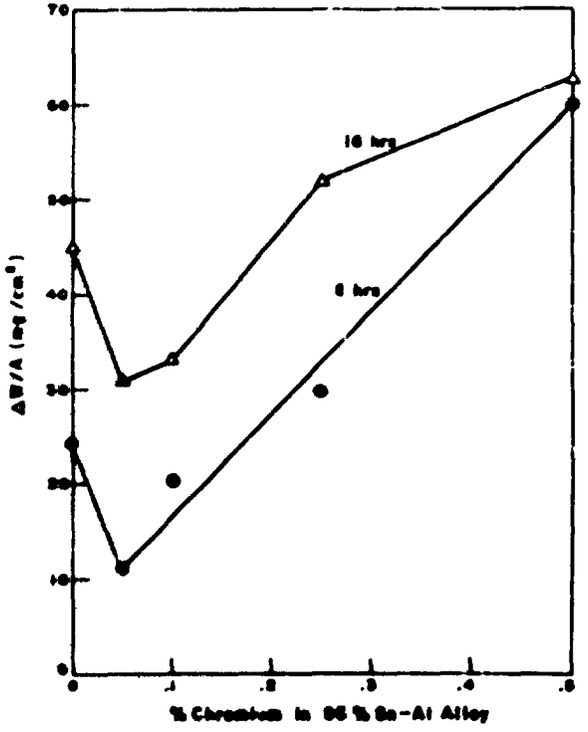

Fig. 16. The effect of chromium additions on the oxidation weight gain of 95% Sn-Al liquid at 1600°C.

5.1 FUTURE STUDIES

During the next report period, additional tests to determine how the additions of chromium influence the oxidation rate at temperatures above 1600°C will be made and tests at lower temperatures will be repeated for verification. In addition, studies of the influence of lanthanum additions to liquid tin-chromium bath alloys will be made to determine if the formation of $AlLaO_3$ perovskite changes the rate of oxidation and to determine the composition of the oxide formed over the multi-component liquid alloy at very high temperatures. Lanthanum has been selected because it also oxidizes to a valence of +3, but in contrast to chromium, tends to stabilize the perovskite structure according to reference 1. Comparisons of the Sn-Al-Ga system with the behavior in the Sn-Al systems at very high temperature should give additional information on the effect of structure and chemical changes on the diffusion rates in oxides.

6. SELECTION OF FUTURE SYSTEMS

The study of the Zr-Th alloy systems and the information previously obtained on the Zr-Nb systems permits an adequate description of the effect of ternary diffusion processes on the layer growth and morphology of oxides formed during the oxidation of an alloy that forms a two-phased oxide. However, the factors that might govern this behavior in the formation of a single-phased oxide such as either a solid solution of halides, or a compound oxide with a definite free energy of formation such as a perovskite, are relatively unknown. During the next report period, several experimental systems will be studied in a preliminary way in order to select one or two useful systems in which the formation of a single-phased alloy or compound oxide grows during oxidation by a diffusion-controlled process. This study should provide additional information on the oxidation of multi-component systems. In addition, systems that demonstrate the effect of the existence of a thermodynamically favored compound oxide on the composition of the oxide formed on liquid substrates will be explored. It is anticipated that two or three new systems will be selected for a more extensive study of the kinetics of oxidation and the tendency for breakaway and for the identification of the structures and compositions of the layers formed on the samples that grow by diffusion-controlled processes.

REFERENCES

1. F. A. Mumpton and R. Roy, "Low Temperature Equilibria Among ZrO_2, TiO_2 and CO_2," J. of the American Ceramic Soc., Vol. 43, 1960, Pg. 234.

2. C. M. Gordon and R. Speiser, "Protection of Niobium Against Oxidation at Elevated Temperatures," Final Report on N60nr-222(28) October 14, 1961.

3. E. J. Rapperport, et al, "Refractory Metal Constitution Diagrams," WADD-TR-60-112, Part II, September 1962.

4. M. O. Nicholas and C. D. Dickinson, "An Analysis of the Basic Factors Involved in the Protection of Tungsten Against Oxidation," ASD-TRD-62-205, Part II, September 1962.

5. Y. Oishi and W. D. Kingery, J. Chem. Phys., 33, 1960, p. 480.

6. J. R. Hensler and E. C. Henry, J. Amer. Ceramic Soc., 36, 1953, p. 76.

7. M. L. Keith and R. Roy, "Structural Relations Among Double Oxides of Trivalent Elements," American Mineralogist, 39, 1954, pp. 1-23.

APPENDIX

COMPOSITIONAL AND STRUCTURAL STUDIES ON THE OXIDATION OF REFRACTORY COMPOUNDS AT HIGH TEMPERATURE

David L. Phalen, Dale A. Vaughan, Neil A. Richard, Alfred E. Austin, and Charles M. Schwartz

Battelle Memorial Institute
Columbus, Ohio

1. INTRODUCTION

Definition of the structure and composition of the phases formed in the oxidation of multicomponent systems is fundamental to an understanding of the role of diffusion processes in the oxidation process. The objectives of Battelle's research program is to establish compositional and structural properties of the oxide layer and residual substrate in several multicomponent systems. The data obtained will aid in predicting diffusion paths and gradients that are produced during the oxidation of these systems.

2. EXPERIMENTAL WORK AND RESULTS

During the period July 1, 1962 to October 1, 1962, the investigation has been limited to the zirconium-thorium-air system. Table A-I gives the compositions of the alloys and the weight-change data resulting from 1200 C exposure to air as provided by General Telephone & Electronics Laboratories, Incorporated. Specimens oxidized for 1/2 hour at 1200°C were supplied for the Battelle studies.

2.1 X-RAY DIFFRACTION TECHNIQUES

Phase compositions through the oxide layer were determined by x-ray diffraction methods. In general, diffractometer recordings were taken at intervals in depth of approximately 1 mil, with successive layers being removed by abrasion on 600-grit silicon carbide paper. Specific particles within the oxide layer were mechanically extracted for analysis by powder diffraction camera methods. The relative intensities of the several diffraction lines for each phase obtained by the diffractometer method differed from those of the powder method. This has been interpreted as indicating preferred orientation in growth of the oxide layer, which unfortunately, prohibited quantitative analysis of the various oxide phases in situ. However, a qualitative analysis of phase composition

TABLE A-I

WEIGHT GAIN OF THORIUM-ZIRCONIUM ALLOYS OXIDIZED AT 1200°C IN DRY AIR

Alloy No.	Composition	Time (hrs)	Weight Gain (g/cm^2)
1	30 w/o Th-Zr	0.25	2.79×10^{-2}
		0.50	4.55×10^{-2}
		1.00	5.55×10^{-2}
2	55 w/o Th-Zr	0.25	1.76×10^{-2}
		0.50	2.32×10^{-2}
		1.00	2.76×10^{-2}
3	70 w/o Th-Zr	0.25	1.19×10^{-2}
		0.50	1.61×10^{-2}
		1.00	1.66×10^{-2}
4	88 w/o Th-Zr	0.25	1.19×10^{-2}
		0.50	1.65×10^{-2}
		1.00	2.03×10^{-2}

The specimens employed in the Battelle studies were oxidized for one-half hour.

was made on the basis of the diffracted intensity for one characteristic line of each phase. Plots of diffracted intensity variations for each phase versus depth below the oxide-air interface are shown in the appended Figs. A-1, A-2 and A-3 for three zirconium-thorium alloys. Since the x-ray beam covers an area of the order of 0.5 cm^2, the data indicate average surface phase compositions rather than discrete particle compositions as analyzed by the electron microprobe method described below.

2.2 ELECTRON MICROPROBE TECHNIQUES

Compositional variations through the oxide layer and down to an equilibrium position in the metal substrate were obtained by electron microprobe analysis of cross sections. Three zirconium alloys containing low, medium, and high thorium contents were studied. Because of the strong interaction of the x-rays, generated by the electron beam of the analyzer, with the elements present in the specimen, the methods for interpreting the raw data are described in some detail.

The characteristic x-ray intensity produced by an element, when a sample is irradiated with an electron beam, is given by the equation:

$$I_a = C_a \int_0^\infty \varphi(\rho_s z) \exp - \left[(\mu/\rho)\, \rho_s z \operatorname{cosec} \phi\right] d(\rho_s z)$$

where I_a is the x-ray intensity; φ is an excitation efficiency function; C_a is the actual mass concentration; μ/ρ is an x-ray mass absorption coefficient, characteristic of both the composition of the sample and the energy of the emitted x-rays; ϕ is the emergence angle of the x-rays from the specimen, and the term ρ_s corresponds to the mass per unit volume of the excited region (~5 $microns^3$) of the sample. It can be seen from this equation that the efficiency of x-ray generation as well as the self-absorption characteristics of the sample are sensitive to the bulk density, ρ_s, of the sample. If the specimen is of uniformly low bulk density, the intensities

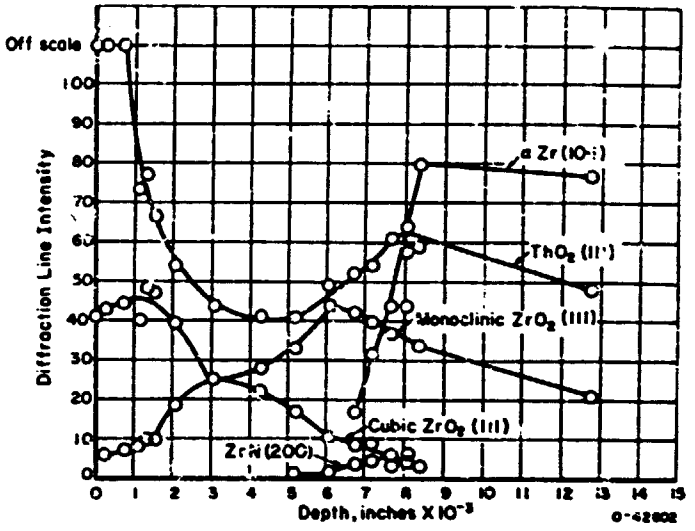

Fig. A-1. Observed diffraction line intensity for various phases versus depth from air-oxide interface.

Alloy No. 1 Zr-30Th

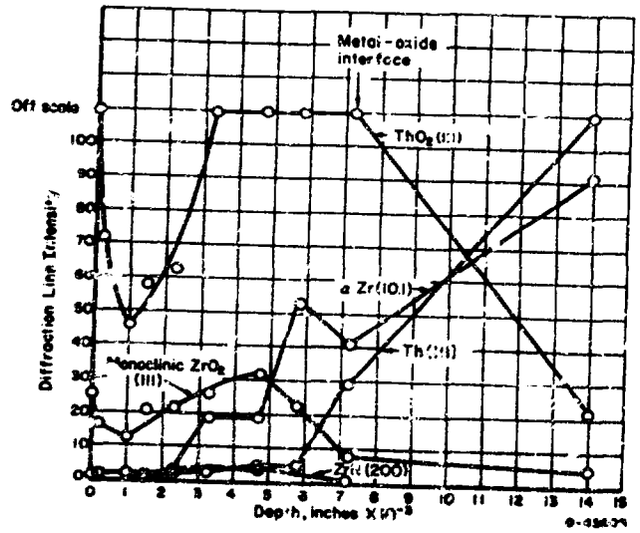

Fig. A-2. Observed diffraction line intensity for various phases versus depth from air-oxide interface.

Alloy No. 2 Zr-55Ti.

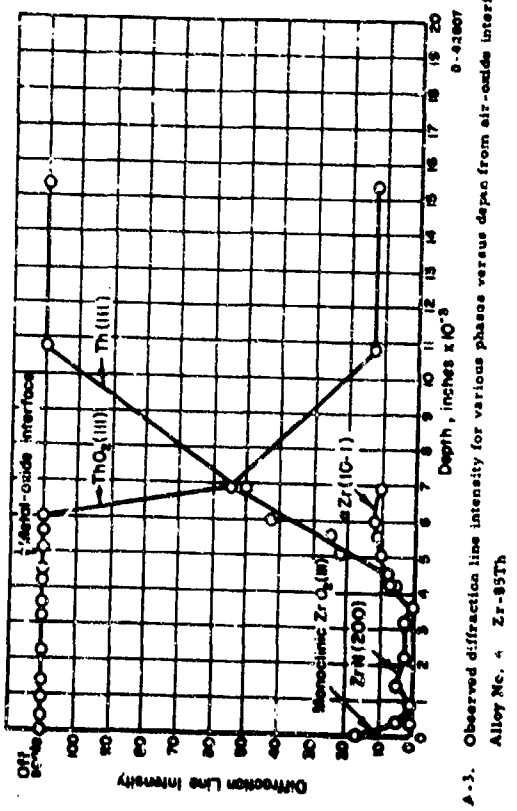

Fig. A-3. Observed diffraction line intensity for various phases versus depth from air--oxide interface.
Alloy No. 4 Zr-85Th

may be adjusted by normalization. Adjustment of the experimental intensities to compensate for large local variations in bulk density, as in the oxide layers of the specimens described here, cannot be carried out with quantitative reliability. However, the data do indicate qualitative and relative changes in composition through the oxide scale. Below the metal-oxide interface the bulk density is not a problem and the data can be treated quantitatively.

The compositional variations through the oxide layers and within specific zones in the base metal, for zirconium alloys containing low, medium, and high thorium contents, are presented graphically in Figs. A-4, A-5, A-6, and A-7. Throughout the base metal the above equation was employed to convert observed intensities, relative to those of pure metals, to weight fractions of the two elements. However, in the case of the oxide scale the characteristic x-ray intensities for zirconium and thorium were measured and then divided by the intensity obtained for pure metallic zirconium and thorium, respectively. These intensity ratios were then converted to weight percent ThO_2 and ZrO_2, based upon the theoretical intensity ratio for dense bodies of the mixed oxides as shown in Fig. A-8. The sharp reversals in the plots for zirconium and thorium content of the oxide scale, as see in Figs. A-4, A-5, A-6, and A-7, are a result of passing from one oxide phase to another. In most cases there appears to be but little solid solubility of ThO_2 in ZrO_2, or vice versa, when the alloys are oxidized at 1200°C.

On the metal side of the metal-oxide interface, the electron probe analyses show the thorium and zirconium content to vary considerably over a distance of approximately 6 mils from the interface. The results show the thorium content to be much lower at the interface than that of the unaffected metal in the central portion of the specimen. A gradient in thorium content is indicated which appears to be uniformly increasing in the Zr-10Th alloy but exhibits some inflections in the other two alloys, alloys are oxidized at 1200°C.

On the metal side of the metal-oxide interface, the electron probe analyses show the thorium and zirconium content to vary considerably over a distance of approximately 6 mils from the interface. The results show the thorium content to be much lower at the interface than that of the unaffected metal in the central portion of the specimen. A gradient in thorium content is indicated which appears to be uniformly increasing in the Zr-10Th alloy but exhibits some inflections in the other two alloys.

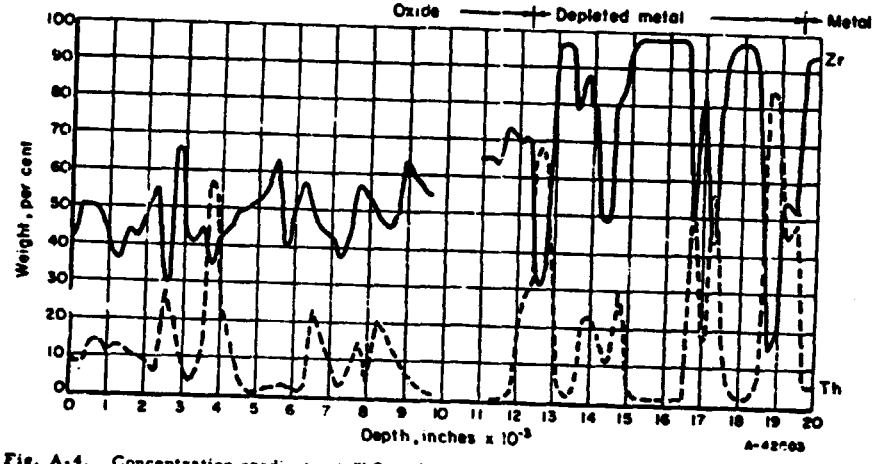

Fig. A-4. Concentration gradients of ThO_2, ZrO_2, Th, and Zr versus depth from air-oxide interface.

Alloy No. 1 Zr-30Th

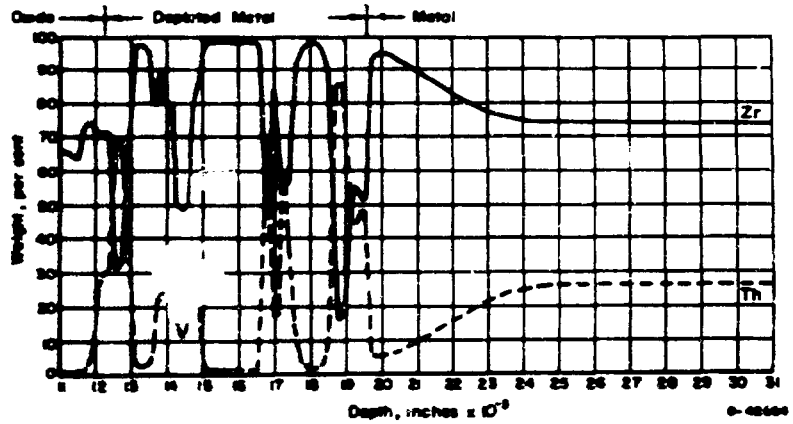

Fig. A-5. Concentration gradients of ThO_2, ZrO_2, Th, and Zr versus depth from air-oxide interface.

Alloy No. 1 Zr-30Th

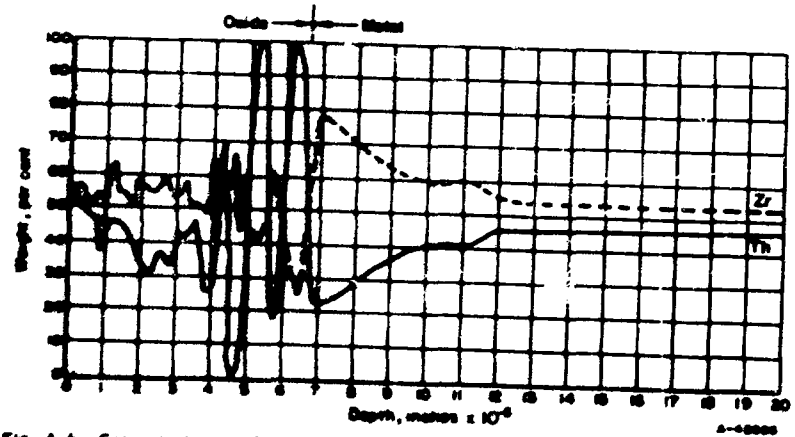

Fig. A-6. Concentration gradients of ThO_2, ZrO_2, Th, and Zr versus depth from air-oxide interface.

Alloy No. 1 Zr-55Th

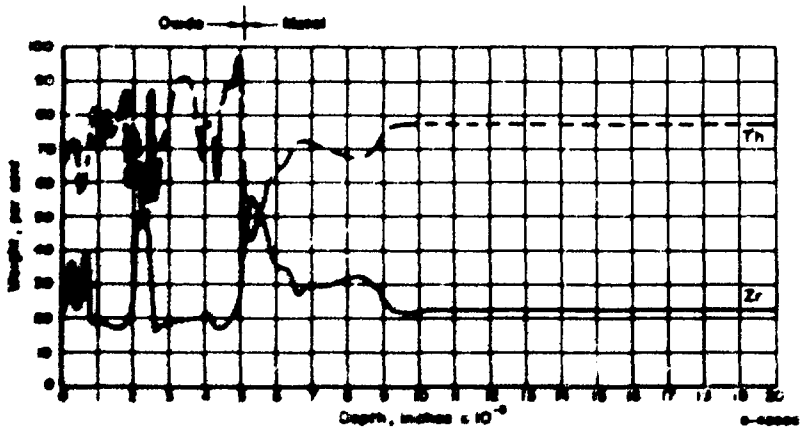

Fig. A-7. Concentration gradients of ThO_2, ZrO_2, Th, and Zr versus depth from air-oxide interface.

Alloy No. 4 Zr-85Th

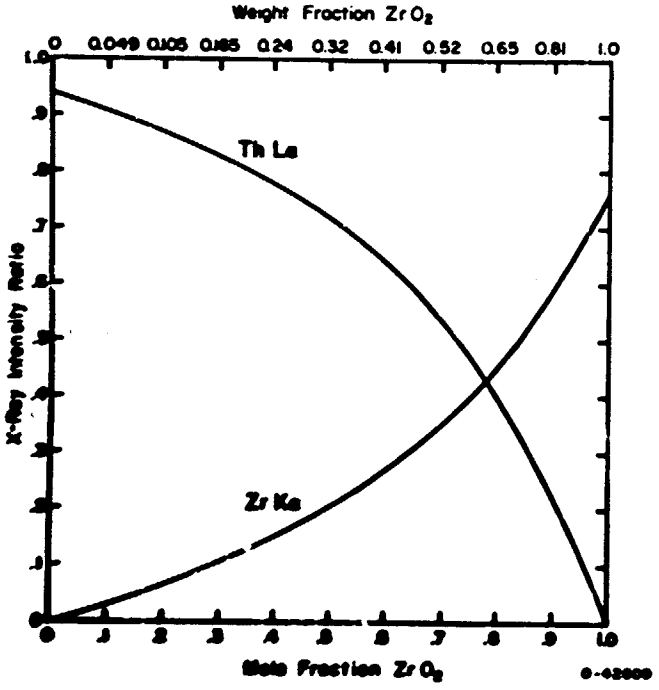

Fig. A-8. Calculated intensity ratios for ThO_2/Th and ZrO_2/Zr versus weight and mole fraction of the mixed oxides.

These inflections are not completely understood. The zirconium content gradient decreases in a corresponding manner.

2.3 METALLOGRAPHIC EXAMINATION

Although in the Battelle program, it is not intended to carry out a complete metallographic study of the specimens under investigation, the electron microprobe analyses are carried out on polished cross sections. Low-power micrographs of polished cross sections (Figs. A-9, A-10 and A-11) were taken to aid in locating reference points while carrying out the microprobe studies and to relate visible discontinuities to the measured compositional changes. In these micrographs, the various phases identified by x-ray diffraction can be observed. The highly reflecting phase in the oxide layer of all three photomicrographs has been identified as ZrN. The matrix of the oxide scale in Fig. A-9 is ZrO_2, while the very dark phase in this photomicrograph is ThO_2. This distribution appears to hold for Fig. A-10 but the ThO_2 particles are smaller and more densely populated. However, in the thorium-rich alloy, shown in Fig. A-11, the matrix of the oxide scale is ThO_2 and the fine particles are ZrO_2. The distribution of the ZrN phase in the oxide scale appears to vary in the three alloys, being near to the metal-oxide interface in the 70Zr-30Th specimen and moving nearer to the air-oxide interface as the thorium content of the alloy is increased. This is confirmed by the x-ray diffraction analyses as shown in Figs. A-1, A-2 and A-3. On the metal side of the oxide-metal interface the oxide phases are dispersed as discrete particles in the metal matrix. The majority of these are ThO_2; however, some ZrO_2 particles were detected in the region near the interface. Electron probe analyses show the metal matrix in this region to be depleted of Th as would be expected to occur when ThO_2 is formed. X-ray diffraction studies of the zirconium phase in this area showed an expanded α-zirconium lattice parameter indicative of a high-oxygen solid-solution.

Fig. A-9. Polished cross-section of zirconium-[illegible] thorium alloy oxidized 1/2 hour at [illegible] in dry air. (100X)

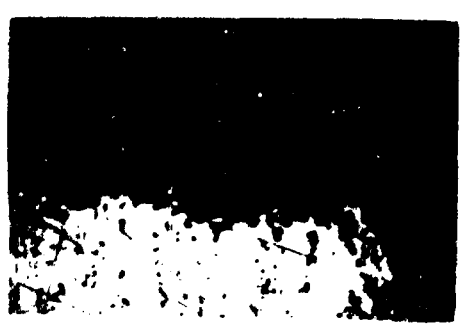

Fig. A-10. Polished cross-section of zirconium-55wt% thorium alloy oxidized 1/2 hour at [illegible] in dry air. (100X)

Fig. A-11. Polished cross-section of zirconium-85 w/o thorium alloy oxidized 1/2 hour at 1200°C in dry air. (240X)

It can be seen from the photomicrographs that the metal-oxide interface is somewhat irregular. As a result difficulties are encountered in attempting to compare electron probe positioning of the interface with respect to that obtained in the x-ray analysis. Since for the x-ray studies the oxide was removed by abrading parallel to the surface, the interface would be observed at the minimum oxide scale thickness. However, the electron probe data were obtained from a position where the oxide layer extends further into the metal. The oxide layer thickness on the 70Zr-30Th alloy varies locally by nearly a factor of 2. This variation is much less in the higher thorium alloys.

3. DISCUSSION OF RESULTS

Structural studies of thorium-zirconium alloys have shown ThO_2, ZrO_2, and ZrN to be the products of oxidation. Of particular interest is the variation in growth characteristics with changes in alloy composition. At the air-oxide interface the degree of preferred orientation decreases with decreasing zirconium content, becoming randomly oriented in 85 wt % thorium alloy. The oxide phases on the 30 wt % thorium alloy become randomly oriented at depth of approximately 3 mils while those on the 55 wt % thorium alloy retain their orientation to a depth greater than 5 mils. It is interesting to note that this change occurs in the 30 wt % thorium alloy at a depth where the amount of cubic ZrO_2 becomes a maximum.

The presence of cubic ZrO_2 in the 30 wt % thorium alloy suggests the possibility that this phase may be stabilized over a large range of temperature by the proper adjustment of the thorium content. However, previous studies at Battelle on the oxidation of pure zirconium have shown that cubic ZrO_2 does form near the metal-oxide interface. This would suggest that the presence of larger amounts of thorium actually destroys

the stability of cubic ZrO_2. This may be due to the loss of coherency between the ZrO_2 and the base metal arising from the abundance of ThO_2 in the oxide scale.

The occurrence of ZrN as an air oxidation product of zirconium is not unusual, but suggests some interesting possibilities in regard to the oxidation mechanism. The oxide scales which have a preferred orientation show a high ZrN concentration near the oxide-metal interface. Possibly, this indicates easier diffusion of the molecular gas (N_2+O_2) through the oriented oxide scale, but more difficult diffusion into the randomly oriented scale of the Zr-85Th alloy. The presence of ZrN and ThO_2 in the absence of ZrO_2, as in the case of the 85 wt % thorium alloy, indicates a strong preference of thorium for oxygen. The higher thorium content is probably sufficient to deplete the air of oxygen leaving nitrogen to react with the zirconium.

An insight into the mechanism of oxidation can be gained by consideration of the elemental and phase composition near the oxide-metal interface. The oxide side is rich in thorium and consists primarily of ThO_2 while the metal side of the interface is lean in thorium, indicating a preferential diffusion and oxidation of thorium across the oxide-metal interface. Also, the thorium is oxidized preferentially by oxygen diffusion into the alloy resulting in the formation of discrete ThO_2 particles in the metal side of the metal-oxide interface. This results in further depletion of thorium from the alloy near the metal-oxide interface. The composition gradients through the affected zone are thus caused by two diffusion processes. It is quite likely that the inflections in these gradients for the medium and high Th alloys is a result of the difference in magnitude of the two diffusion reactions. However, the effect of oxygen solid solution on the phase equilibrium in the Zr-Th system is unknown except that oxygen stabilizes the hexagonal structure to higher temperatures. Thus the inflections in compositional gradients may be due to phase boundaries in the Zr-Th-O system.

4. CONCLUSIONS

During the period July 1, 1962 to October 1, 1962, x-ray diffraction, electron microprobe and metallographic analysis of 30, 55, and 85 wt % thorium-zirconium alloys oxidized one-half hour at 1200°C in dry air have been studied. The results to date have shown that:

1. Oxidation products of thorium-zirconium alloys are ThO_2, ZrO_2, and ZrN.
2. Both the monoclinic and cubic forms of ZrO_2 are observed in Zr-30 wt % thorium alloys, but only monoclinic ZrO_2 in Zr-55Th and Zr-85Th alloys.
3. The location of ZrN varies with composition of the alloys, being modified by the magnitude of the oxygen gettering action of thorium.
4. Preferred orientation of the oxides is exhibited in those alloys containing medium and low concentrations of thorium.
5. Preferred orientation of the oxides persists to a greater depth in the 55 wt % thorium alloy than in the low or high thorium alloys.
6. The oxidation mechanism of thorium-zirconium alloys is one of air diffusion in which thorium is oxidized first; the zirconium then becomes supersaturated with oxygen precipitating ZrO_2, but if a deficiency of oxygen occurs ZrN forms.
7. ZrN appears to be oxidation resistant at 1200°C.

8. Compositional gradients are produced in the metal substrate as a result of two diffusion processes: oxygen inward and thorium outward.

5. FUTURE WORK

In the immediate future our efforts will be directed toward a study of the zirconium-70 wt % thorium alloy. Upon receipt of new specimens from General Telephone and Electronics Laboratories, the specimens will be analyzed by x-ray diffraction and electron microprobe methods.

END